Nucleon-nucleus reactions at ultrarelativistic energies

Cheuk-Yin Wong
Oak Ridge National Laboratory, Oak Ridge, Tennessee
(Received 18 June 1984; revised manuscript received 11 March 1985)

In order to discern coherent processes from incoherent and collective processes in nucleon-nucleus reactions at high energies, we study these reactions with an incoherent-multiple-collision model. In this model, the projectile nucleon makes successive inelastic collisions with nucleons in the target nucleus, the probability of such collisions being given by the thickness function and the nucleon-nucleon inelastic cross section. It is assumed that each baryon-baryon collision produces particles and degrades momenta just as a baryon-baryon collision in free space, and that there are no secondary collisions between the produced particles and the nucleons. We found that the inelastic proton data, the pseudorapidity distribution data $dN^{pA}/d\eta$, and the total nucleon-nucleus absorption data can be well explained by the incoherent-multiple-collision model. However, the single-particle fragmentation data for nonleading particles indicate that there is a reduction of the fragmentation cross section because of subsequent collisions of the leading baryon along the collision chain. Modification of the incoherent-multiple-collision model is suggested. The modified model gives cross sections for the reactions $pA \to \pi^+ X$, $pA \to \pi^- X$, $pA \to K^+ X$, $pA \to K^- X$, and $pA \to \bar{p} X$ in the projectile fragmentation region in good agreement with experiment.

I. INTRODUCTION

Recently, there is much interest in relativistic nucleus-nucleus collisions, which have been suggested as a possible way to produce a phase transition from ordinary confined matter to unconfined quark-gluon plasma.[1-7] Experimental searches and investigations of the quark-gluon plasma will provide a new insight into the mechanism of quark confinement. It will also allow one to study the properties of the primordial matter which existed in the early Universe.[8]

The energy density of the produced particles and the baryon rapidity distribution shortly after a nucleus-nucleus collision can be studied by using a multiple-collision model[7,9-11] in which the basic process is the nucleon-nucleon or the baryon-baryon collision. We would like to examine the multiple-collision model further to assess whether the model is approximately valid for some restricted regions of phase space. As the model is parameter free, we also wish to use the model as a reference model whereby coherent effects in some other regions of phase space may be discerned as systematic deviations.

While many multiple-collision models[9-18] have been employed in the past, it is worthwhile to spell out the assumptions involved in the version of the multiple-collision model[7,9,10] we shall examine. In a multiple-collision model, a nucleon in one nucleus makes many inelastic collisions with nucleons in the other nucleus, the probability of collision being given by the thickness function[11] and the total nucleon-nucleon inelastic cross section. (In this description, as an elastic collision has negligible contributions to energy degradation and particle production, we shall ignore elastic collisions altogether. Henceforth, by a nucleon-nucleon or a baryon-baryon collision, we shall mean a nucleon-nucleon inelastic or a baryon-baryon inelastic collision, respectively.) The nucleon may change its identity during its passage through the nucleus, but its baryon number remains unchanged. The relation between the Glauber multiple-collision expansion and the high-order Feynman diagrams in a hadron-nucleus collision was first demonstrated by Gribov and studied further by other authors.[12,14] The multiple-collision model is a reasonable description if the range of the nucleon-nucleon interaction is short compared with the spacing between nucleons. In the laboratory frame, the latter quantity is of the order of 2 fm, while the range of the nucleon-nucleon interaction is about 0.7 fm and decreases with increasing energy. It appears that a multiple-collision model may be a reasonable concept. Indeed, the Glauber model gives the correct total pA absorption cross section and the correct mass dependence.[19] A Glauber model with the assumption of no secondary collisions but no adjustable parameters gives the rapidity density in the central rapidity region consistently[7,20] within 30%, while a phenomenological Glauber model with an adjustable parameter to take into account effectively energy degradation improves the agreement[7] with experiment to within about 5%. A multiple-collision picture of the Glauber type appears to have approximate validity in describing the gross features of the reaction process. However, there are complications when we try to examine the finer details of high-energy nucleus-nucleus collisions. In these collisions most of the particles are produced outside the nuclei,[21] while energies of the baryons are apparently degraded inside the nucleus. One can construct a schematic picture similar to those in Refs. 14—16 to describe how this can proceed (Fig. 1). In the nucleus-nucleus collision, the nucleons of one nucleus may or may not collide with nucleons of another nucleus. If an inelastic collision occurs, there is a degradation in energy and a production of particles. To describe this degradation and particle production, one can associate the

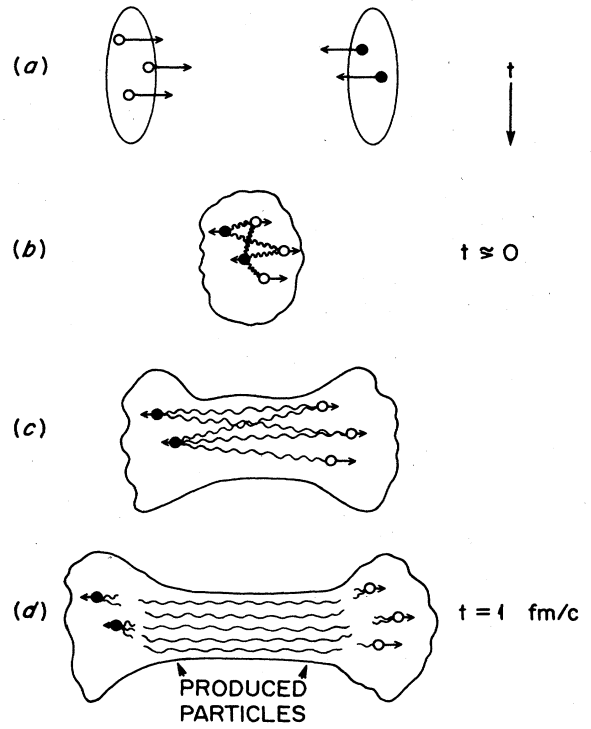

FIG. 1. Schematic representation of a nucleus-nucleus collision in the multiple-collision model. (a) shows the configuration of the colliding nuclei before collision; the lengths of the arrows indicate the momenta of the nucleons. Nucleons in the left nucleus are shown as open circles, while those in the right nucleus are shown as solid circles. (b) shows the configuration shortly after the collision. The momenta are degraded and a string indicated by a curvy line is developed between the collided nucleons. In (c), the baryons travel forward and the strings are stretched. At a time of about 1 fm/c, in the center-of-mass system after the collision (d), the strings are broken and particles are produced in the central rapidity region.

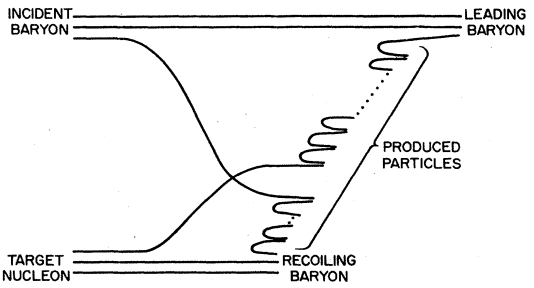

FIG. 2. Possible microscopic description of the string of Fig. 1. An incident nucleon makes an inelastic collision with a target nucleon when one of its valence quarks collides with a valence quark of the target nucleon. The spectator quarks of the incident baryon hadronize instantaneously to form a leading baryon and continue to collide with other target nucleons. The curly-bracketed section is a representation of the string of Fig. 1. Particles are produced when the leading baryon and the recoil baryon are about 1 fm apart (in the center-of-mass system).

development of a string between the collided baryons[22] with each inelastic baryon-baryon collision [Fig. 1(b)]. The development of string degrades the momenta of the colliding nucleon. To describe particle production outside the nuclei, one can associate the production process to occur when the string is stretched to a length of about 1 fm in the center-of-mass system[1] [Fig. 1(d)]. Finally, to describe independent baryon-baryon collisions and no secondary collisions of the produced particles, one can ascribe the development of the strings to be independent of each other. At ultrarelativistic energies, the strings are likely to be parallel to each other and shadowed by the leading particle so that there is no collision among the strings and between the strings and the nucleons. While the exact nature of the string is not yet resolved, a possible description of the string can be given in terms of the dual parton model[23] of the constituent quarks (Fig. 2). We envisage that an incident nucleon suffers an inelastic scattering when one of its valence quarks collides with a valence quark of the target nucleon. The two other spectator quarks proceed forward and, together with a quark q from the $q\bar{q}$ polarization, form a color-singlet baryon to make further collisions with nucleons along its path. The section indicated by the curly brackets in Fig. 2 can be a representation of the string of Fig. 1.

The above schematic picture is useful for illustrative purposes. For a quantitative analysis, it is necessary to know how the energies of the baryons are degraded as they pass through the other nucleus and how the degradation of energy affects the production processes. Different assumptions will lead to different models and results.

In this paper, we undertake to study a simple parameter-free version of the multiple-collision model. In the target frame, the separation between nucleons is much greater than the range of nucleon-nucleon interactions. It is plausible that the string that is developed in an earlier baryon-baryon collision is not much influenced by later collisions. To a first approximation, then, this small influence can be neglected and included later only as corrections. One then has a multiple-collision model in which each nucleon-nucleon or baryon-baryon inelastic collision produces particles and degrades the energies and the momenta of the colliding nucleons (or baryons) in the same way as baryon-baryon inelastic collision in free space. In this description, a nucleus-nucleus collision consists of a collection of successive incoherent elementary baryon-baryon collisions. The momentum distribution of the resultant leading baryon is obtained by folding the momentum distributions of all its previous collisions. As particles are mostly produced outside the nuclei,[21] we make the further assumption of no secondary collisions between the produced hadrons and the target or projectile nucleons. Then the rapidity distribution of the produced hadrons is just an additive superposition from all the nucleon-nucleon or baryon-baryon collisions. Implicit in this model is the assumption of a local character of the baryon conservation during each baryon-baryon collision. Recent experimental data on the correlation of produced baryon pairs suggests that baryon conservation may be local in character.[24]

In this paper, we specialize in the simple case of nucleon-nucleus scattering and examine many types of data. They include the single-particle inclusive fragmentation data[25,26] for $pA \to pX$, $pA \to \pi^+ X$, $pA \to \pi^- X$, $pA \to K^+ X$, $pA \to K^- X$, and $pA \to \bar{p} X$, the particle-production data[20] $dN^{pA}/d\eta$, and the total-pA-absorption-cross-section data.[19] A subset of the above has been analyzed by various authors[23,27–37] using various models. We would like to know whether there is any basis for the estimates of the initial energy density of quark-gluon plasma in nucleus-nucleus collisions presented previously in Ref. 7.

The multiple-collision model we have postulated is by itself physically plausible, but its development will also serve other useful purposes. In this phenomenological model, all the baryon-baryon collisions are independent, and their effects are incoherently superimposed. If the baryon-baryon data are known, there will be no free parameters; all the information must come from the relevant nucleon-nucleon (or baryon-baryon) experimental data. It does not include coherent effects such as arising from the interference due to later baryon-baryon collisions, the mean-field hydrodynamical-type compression,[38] the formation-zone effect of Landau and Pomeranchuk,[39] inside-outside-cascade effects,[40] and the effects due to the formation of the quark-gluon plasma, etc. Furthermore, the assumption of an energy loss per collision the same as if in free space is one of simplicity and may need to be modified. It may turn out to be reasonable if from one collision to the next the creation of the string leads to a loss of the energy of the leading particle almost as large as the asymptotic energy loss. It may also turn out otherwise, and future analyses may require knowledge of the fraction of the asymptotic energy loss as the chain of collisions proceeds. This multiple-collision model with no free parameters can serve as a reference model (a benchmark, so to speak) whereby any coherent or other effect, if it exists at all, may manifest itself as systematic deviations of the experimental data from model predictions. It is important to test the model in cases where there are experimental data available, not only to judge the approximate validity of the model, but also to see if there is any need for the introduction of additional corrections or modifications due to coherent or other effects.

The need for a reference model is all the more compelling in view of recent interest in the production of a quark-gluon plasma by heavy-ion collisions.[1–7] To identify the presence of a quark-gluon plasma, it is necessary to probe the system by detecting various particles.[4] The same particles are produced by the incoherent process of nucleon-nucleon collisions. The signal from quark-gluon plasma must be compared with and contrasted against the production of the same particles in incoherent processes. Hence, it is useful to develop an accurate reference model of incoherent multiple collisions to aid the detection of the quark-gluon plasma.

The Glauber-type multiple-collision model we have postulated is an extension of the model of Blankenbecler *et al.*[13] to include additional assumptions concerning energy degradation and particle production. The model is similar to the multichain model[14–16] but has important differences in treatment methods and the use of approximations. In particular, in the multichain model the momentum distribution of the colliding baryons comes from a coherent but unknown partition of the energy among the collision chains. In Ref. 15, it is given by a postulated probability function $P(\lambda)=\alpha\lambda^{\alpha-1}$, where α is a free parameter and found to be ~ 6. In some other work on the multichain model,[16] the momentum distribution is parametrized in terms of an equal partition of the beam momentum among the arms of the chain. However, there are many approximations in the numerical calculations which make their conclusions uncertain. In contrast, we obtain the momentum distribution from nucleon-nucleon experimental data, and a realistic nuclear density is used.[9,10] The model is similar to the model of Vary and co-workers[17] but has also important differences. There, the probability of a nucleon-nucleon collision leading to particle production is assumed to be given by the *total* nucleon-nucleon cross section multiplied by the normalized thickness function. In contrast, we consider particle production to occur only in *inelastic* collisions. Our model differs from the multiple-collision model of Ref. 18 in the same respect. There are, in addition, other differences in the use of kinematic constraints and experimental information of the stopping power.

A subset of the data we shall examine has been analyzed previously by many authors in addition to those mentioned above.[7,9,15,16] Some recent theoretical work[28] studied $pA \to pX$ data in terms of a basic degradation function involving an adjustable parameter and a postulated relation of $A^{2/3}$ between the invariant pA cross section and the mass number A. Recently Csernai and Kapusta[29] studied the same reaction but made the postulate that a proton remains a proton throughout the collision chain, and adjusted arbitrary parameters to fit experimental data. Such an analysis is subject to question. In a pp collision, there is only a probability of about 60% for the leading baryon to remain a proton.[26] The postulate of a proton remaining to be a proton throughout the collision chain may lead to misleading results. Recent work by Hüfner and Klar[30] and Daté, Gyulassy, and Sumiyoshi[31] adopted an approach similar to that of Ref. 15.

Some recent work[32] on the distribution dN^{pA}/dy in proton-nucleus collisions made use of a phenomenological model where two phenomenological functions $\rho_0(y)$ and $\beta(y)$ were adjusted to describe dN^{pA}/dy. Although good fits to the data were obtained, it is desirable to explain the data in terms of known quantities without adjustable functions. There are many other theoretical models which analyze the rapidity distribution dN^{pA}/dy. (See Refs. 24 and 33 for a review of various models.) The energy-flux-cascade model[34] assumes the propagation of an energy flux which is divided into slices in the rapidity space. The original energy-flux-cascade model does not give agreement with experiment. Agreement can be obtained by modifying the way the rapidity space is to be sliced. However, the underlying physics as to how this division is made is not obvious.[33] The additive quark model[35,36] and the dual parton model[23,24] assumes a quark-parton description of the hadrons. In the additive quark model, only the valence quarks can interact, but in

the dual parton model, both the valence quarks and the sea quarks can interact. Both models are successful in describing the production of particles in the central rapidity region. Whether it can also describe the production of p, $\pi^{\pm}$, $K^{\pm}$, and $\bar{p}$ in the fragmentation region is not known.

Other previous work by Brodsky, Gunion, and Kühn[37] on hadron production in nucleon-nucleus collisions is described in terms of the interaction of the wee quark partons on the projectile with the wee quark partons of the target. The rapidity location of the parton-parton collision is postulated to be uniformly distributed in the central region. The height of the multiplicity plateau is also assumed to be independent of the number of collisions the projectile parton has suffered. These assumptions are not justified from the consideration of energy-momentum conservation of nucleon-nucleon collision data. It is not surprising that, although the model gives reasonable agreement with the ratio of total multiplicities in nucleon-nucleus collisions, it can give only a qualitative, but not quantitative, description of the asymmetric shape of dN^{pA}/dy. Furthermore, its generalization to nucleus-nucleus collisions gives multiplicities too low by a factor of 2 (Ref. 4).

It is instructive to rephrase our multiple-collision model in the language of the parton model of nucleon partons (and not quark partons). As is emphasized not the least by Schmidt and Blankenbecler,[41] nucleons are partons in a nucleus. In our model, the nucleon partons of the target nucleus collide with the projectile nucleon partons, and the partons lose energy and momenta and produce hadrons in each parton-parton collision in accordance with the parton-parton collision data in free space. Written in this parton-model language, our model differs from that of Brodsky, Gunion, and Kühn[37] in the specific nature of partons, in the way the partons degrade in energy and in the way hadrons are produced. Namely, nucleons are partons in our model, and the rapidity locations of the parton-parton collision are not uniformly distributed but are given by parton-parton experimental data. The height of the multiplicity plateau is not constant but becomes lower in subsequent collisions as determined by parton-parton data. The width of the plateau for each parton-parton collision also depends on parton-parton relative energy at the moment of collision.

Returning to the language of baryon-baryon collisions, we can follow the incident baryon in the collision chain. In each baryon-baryon inelastic collision, the rapidity distribution of the produced particles depends on the center-of-mass energy of the two colliding baryons. As the fractional loss of energy per nucleon-nucleon collision is not small,[9,10,27] the magnitudes of the distributions of multiplicity dN/dy due to each subsequent collision of a nucleon are lower than those due to the first collision. These distributions also shift toward the target rapidly. It is important to follow the energy of the baryon as it traverses the target nucleus. For this purpose, we shall include the transverse-momentum distribution in a factorizable approximation in which the longitudinal and the transverse degrees of freedom are separable. The total rapidity distribution of the produced particles can then be obtained by simple numerical integrations.

This paper is organized as follows. In Sec. II, we generalize our results on the momentum distribution of an incident baryon after n successive collisions[9] to include also the transverse-momentum distribution in the factorizable approximation. In Sec. III, we use these new results to obtain the invariant $pA \to pX$ cross sections which are then compared with the experimental data of Barton *et al.*,[25] Eichten *et al.*,[42] and Allaby *et al.*[43] We examine in Sec. IV the stopping power of a baryon in a nucleus with the inclusion of the transverse momentum distribution and kinematic constraints. The average rapidity of a baryon $\bar{y}_n$ after n successive collisions is obtained numerically. Knowing the average rapidity, we calculate the center-of-mass energy before the next baryon-baryon collision. The rapidity distribution of the produced hadrons in each baryon-baryon collision is extrapolated from nucleon-nucleon data to give the total distributions of the produced particles in Sec. V. They are compared with the experimental $dN^{pA}/d\eta$ data of Elias *et al.*[20] In Sec. VI we investigate single-particle cross sections for the production of nonleading particles in the incoherent-multiple-collision model. A general result applicable to all regions of rapidity space is obtained. In Sec. VII, we specialize to the projectile fragmentation region and the reactions of $pA \to \pi^+ X$ and $pA \to \pi^- X$. The theoretical results are compared with the experimental data of Barton *et al.*[25] Systematic deviations of the predictions of the incoherent-multiple-collision model from experimental data indicate the presence of coherent effects. A phenomenological reduction factor which depends on the number of subsequent collisions is introduced to explain the data. In Sec. VIII we study the fragmentation reactions in the first-collision approximation in which the nonleading particles come from the first of many collisions of the incident nucleon. We analyze the cross sections for the reactions of $pA \to K^+ X$, $pA \to K^- X$, and $pA \to \bar{p} X$ in this approximation. How one incorporates the reduction factor to study particle production in the central rapidity region is discussed in Sec. IX. Section X summarizes the present discussions.

II. MOMENTUM DISTRIBUTION AFTER n INELASTIC COLLISIONS

In the multiple-collision model, the basic process is the baryon-baryon collision. The baryon-baryon inelastic collision data provides the basic information from which other results are obtained. We can parametrize the $pp \to pX$ data in the form

$$E\frac{d\sigma}{dp^3} = x\frac{d\sigma}{dx}\frac{1}{2\pi\sigma_t}\exp(-p_t^2/2\sigma_t^2) , \tag{2.1}$$

where x is the Feynman scaling variable defined by

$$x = \frac{c_0 + c_z}{b_0 + b_z} , \tag{2.2}$$

with c_0 and c_z, respectively, the energy and the longitudinal momentum of the detected particle c (proton in this case) and b_0 and b_z, respectively, the energy and the long-

itudinal momentum of the beam particle (incident proton in this case). In terms of the Feynman scaling variable, the three-momentum of a baryon $\mathbf{p}$ can be represented by $(x,\mathbf{p}_t)$. The standard deviation σ_t in the transverse momentum $\mathbf{p}_t$ is a function of x (Ref. 26). It equals 0.28 GeV/c at $x=0.8$, 0.31 GeV/c at $x=0.5$, and 0.35 GeV/c at $x=0.3$. For simplicity, we shall make the factorizable approximation of assuming a constant average σ_t ($\sigma_t=0.31$ GeV/c in this case) for all values of x. We also assume that the invariant cross section of $pp\to pX$ is related to that of $bb\to bX$, where b is a baryon, by a constant branching factor. The momentum distribution of the incident nucleon (or baryon) *after* n inelastic collisions $D^{(n)}(x_n,\mathbf{p}_{tn})$ is connected with that after $(n-1)$ inelastic collisions $D^{(n-1)}(x_{n-1},\mathbf{p}_{t\,n-1})$ by

$$D^{(n)}(x_n,\mathbf{p}_{tn})=\int dx_{n-1}d\mathbf{p}_{t\,n-1}D^{(n-1)}(x_{n-1},\mathbf{p}_{t\,n-1}) \times w(x_{n-1},\mathbf{p}_{t\,n-1};x_n,\mathbf{p}_{tn}) , \tag{2.3}$$

where the function $w(x_{n-1},\mathbf{p}_{t\,n-1};x_n,\mathbf{p}_{tn})$ is the probability distribution for finding a "leading" baryon with a final Feynman scaling variable x_n and a transverse momentum $\mathbf{p}_{tn}$ after a nucleon-nucleon or a baryon-baryon inelastic collision if the initial scaling variable is x_{n-1} and the initial transverse momentum is $\mathbf{p}_{t\,n-1}$. Experimental data at a fixed $\mathbf{p}_t$ for $pp\to pX$ reactions at high energies show a nearly flat[26] and energy-independent[44] differential cross section as a function of the Feynman scaling variable x. There is a quasielastic diffractive peak around $x=1$. Its contribution to the total $pp\to pX$ inelastic cross section (over and above the nearly flat distribution) is about 6%. Thus, one can approximately express the nucleon-nucleon inelastic differential cross section $d\sigma/dx$ as the sum of a "truly" inelastic part λ and a quasielastic part $1-\lambda$

$$\frac{d\sigma}{dx}=[\lambda\theta(1-x)\theta(x-x_L)+(1-\lambda)\delta(1-x)]\sigma_R , \tag{2.4}$$

where $\lambda=0.94$, x_L is the lower limit of x in accordance with energy-momentum conservation, and σ_R is the total nucleon-nucleon reaction cross section.

From the differential cross section (2.4) and Eq. (2.1), we can write the normalized probability distribution w as given by

$$w(x_{n-1},\mathbf{p}_{t\,n-1};x_n,\mathbf{p}_{tn})=\left[\lambda\frac{\theta(x_{n-1}-x_n)\theta(x_n-x_L)}{x_{n-1}-x_L}+(1-\lambda)\delta(x_n-x_{n-1})\right]F^{(n)}(\mathbf{p}_{t\,n-1},\mathbf{p}_{tn}) . \tag{2.5}$$

How the transverse momentum of the leading particle varies as it traverses the nucleus is not completely understood. There are two possibilities. One can envisage the leading particle to maintain its identity as it travels through the nucleus, and that the particle suffers a transverse-momentum kick during each baryon-baryon collision. In this case the transverse momentum of the leading particle after the nth collision is the vector sum of that after the $(n-1)$th collision and the transverse momentum due to the collision. The function $F^{(n)}$ is then

$$F^{(n)}(\mathbf{p}_{t\,n-1},\mathbf{p}_{tn})=\frac{1}{2\pi\sigma_t^{\,2}}\exp\left[\frac{(\mathbf{p}_{tn}-\mathbf{p}_{t\,n-1})^2}{2\sigma_t^{\,2}}\right] . \tag{2.6}$$

In this case, the width of the transverse momentum after n collisions, σ_{tn}, grows with n as $\sqrt{n}\,\sigma_t$. We call it the case of an increasing transverse (-momentum) width.

There is another possibility. If the leading particle suffers such a large loss of energy that the leading particle is the remnant of an inelastic nucleon-nucleon collision. That is, the leading baryon is itself a product of a previous collision. In that case, there is a natural frame of reference for the nth collision in which the z axis in that frame lies in the direction of the momentum of the leading particle before the nth collision. The angle of rotation between the natural frame of reference and the laboratory frame is very small due to the large value of the longitudinal momentum in comparison to the transverse momentum. Thus, even though the leading particle has a transverse momentum, it travels essentially in the beam direction and thus produces a subsequent leading particle with essentially the same transverse-momentum width.[45] In this case, which we call the case of a constant transverse (-momentum) width, the function $F^{(n)}(\mathbf{p}_{tn},\mathbf{p}_{t\,n-1})$ is

$$F^{(n)}(\mathbf{p}_{t\,n-1},\mathbf{p}_{tn})=\begin{cases}\dfrac{1}{2\pi\sigma_t^{\,2}}\exp\left[-\dfrac{(\mathbf{p}_{tn}-\mathbf{p}_{t\,n-1})^2}{2\sigma_t^{\,2}}\right] & \text{for } n=1\\ \delta(\mathbf{p}_{tn}-\mathbf{p}_{n-1}) & \text{for } n\geq 2 .\end{cases} \tag{2.7}$$

The distributions $D^{(n)}$ and w are normalized according to

$$\int D^{(n)}(x_n,\mathbf{p}_{tn})dx_n d\mathbf{p}_{tn} = \int w(x_{n-1},\mathbf{p}_{t\,n-1};x_n,\mathbf{p}_{tn})dx\,d\mathbf{p}_{tn}=1 . \tag{2.8}$$

Explicitly, x_L in Eq. (2.5) is given by[10]

$$x_L=\left[\frac{m_T}{m}\right]^2\frac{m}{(b_0+b_z)_{\text{lab}}} , \tag{2.9}$$

where

$$m_T=(m^2+\mathbf{p}_t^{\,2})^{1/2} , \tag{2.10}$$

m is the nucleon mass, and b_0 and b_z are the energy and the longitudinal momentum of the incident beam particle. With x_L depending on $\mathbf{p}_t$, the longitudinal and the transverse degrees of freedom are not separable. We shall make the separable approximation in which the $\mathbf{p}_t^{\,2}$ in Eq. (2.10) is replaced by its expectation value *after* collision. This is a reasonable approximation, as the transverse momentum is relatively sharply peaked for small values of n, and the average value of n for collisions with even the heaviest target is approximately 4.

Initially, the momentum distribution is

$$D^{(0)}(x,\mathbf{p}_t)=\delta(x-1)\delta(\mathbf{p}_t) . \tag{2.11}$$

If the δ-function term in Eqs. (2.4) and (2.5) is absent, a properly normalized w function will lead to a distribution

$$D^{(n)}(x,\mathbf{p}_t) = \frac{\theta(1-x)}{1-x_L(n)}\frac{\theta[x-x_L(n)]}{(n-1)!}\left[-\ln\left[\frac{x-x_L(n)}{1-x_L(n)}\right]\right]^{n-1} \times\frac{1}{2\pi\sigma_{tn}^{\,2}}\exp\left[-\frac{p_t^{\,2}}{2\pi\sigma_{tn}^{\,2}}\right], \tag{2.12}$$

where $x_L(i)$ is the lower limit of x after i collisions

$$x_L(i)=(1+2\sigma_{ti}^{\,2}/m^2)^{1/2}m/(b_0+b_z)_{\rm lab}\ .$$

For the case of an increasing transverse-momentum width, the transverse-momentum width is related to the collision number n by

$$\sigma_{tn}^{\,2}=n\sigma_t^{\,2}\ . \tag{2.13}$$

For the other case of a constant transverse width, the transverse-momentum width is independent of the number of collisions,

$$\sigma_{tn}^{\,2}=\sigma_t^{\,2}\ . \tag{2.14}$$

Our previous analysis[10] of the $pA\to pX$ data used implicitly the assumption of a constant transverse width [cf. Eq. (6.17) of Ref. 10].

We denote by $\tilde{D}^{(n)}$ the distribution function after n collisions obtained when the δ-function term in Eqs. (2.4) and (2.4) for elastic and quasielastic scattering is present. Clearly, $\tilde{D}^{(0)}=D^{(0)}$. For $n=1$, we have

$$\tilde{D}^{(1)}(x,\mathbf{p}_t)=\left[\lambda\frac{\theta(1-x)\theta(x-x_L(1))}{1-x_L(1)}+(1-\lambda)\delta(1-x)\right] \times\frac{1}{2\pi\sigma_t^{\,2}}\exp\left[-\frac{\mathbf{p}_t^{\,2}}{2\sigma_t^{\,2}}\right]. \tag{2.15}$$

In general, we have

$$\tilde{D}^{(n)}(x,\mathbf{p}_t)=\left[\sum_{i=0}^{n}\binom{n}{i}\lambda^i(1-\lambda)^{n-i}D^{(i)}(x,\mathbf{p}_t)\right], \tag{2.16}$$

where $D^{(i)}$ is given by Eq. (2.12).

There is a simplification which we shall make. As far as energy degradation and particle production are concerned, elastic and quasielastic scatterings give negligible degradation and particle production. In fact, in the approximate form to represent elastic and quasielastic scatterings by a δ function as in Eq. (2.4), they give no contribution at all. Anticipating the result of Eq. (3.4) in the next section, we can prove the identity that

$$\sum_{n=0}^{A}\binom{A}{n}\tilde{D}^{(n)}(x,\mathbf{p}_t)(T_A\sigma_R)^n(1-T_A\sigma_R)^{A-n} =\sum_{n=0}^{A}\binom{A}{n}D^{(n)}(x,\mathbf{p}_t)(T_A\lambda\sigma_R)^n(1-T_A\lambda\sigma_R)^{A-n}\ , \tag{2.17}$$

where T_A is the thickness function of the target nucleus A. This identity shows that as far as inelastic scattering (i.e., terms with $n\geq 1$) is concerned, the result obtained with the total reaction cross section σ_R and the corresponding distributions $\tilde{D}^{(n)}$ is the same as that using only the distributions $D^{(n)}$ in conjunction with a truly inelastic nucleon-nucleon collision with the cross section $\sigma_{\rm in}$:

$$\frac{d\sigma}{dx}=\sigma_{\rm in}\theta(1-x)\theta(x-x_L)\ , \tag{2.18}$$

with $\sigma_{\rm in}$ given by

$$\sigma_{\rm in}=\lambda\sigma_R\ . \tag{2.19}$$

Henceforth, we shall use the distribution $D^{(n)}$ and the corresponding $\sigma_{\rm in}$ in our subsequent discussions. Experimentally, the reaction cross section σ_R for pp collisions[25] is 31.3 mb. Thus, the total cross section $\sigma_{\rm in}$ for the (truly) inelastic pp collision is 29.4 mb, which can be taken to be also the cross section for truly inelastic baryon-baryon collisions.

Besides the Feynman scaling variable x, there is a complementary rapidity variable y defined by

$$y=\tfrac{1}{2}\ln\frac{c_0+c_z}{c_0-c_z}\ , \tag{2.20}$$

where c is the momentum of the baryon particle in question. Therefore x and y are related by

$$\ln x=y-y_B+\ln(m_{cT}/m)\ , \tag{2.21}$$

where

$$m_{cT}=(m_c^{\,2}+c_t^{\,2})^{1/2}\ , \tag{2.22}$$

m_c is the mass of detected particle c, and y_B is the rapidity of the incident (beam) particle. In terms of the rapidity variable, the three-momentum vector $\mathbf{p}$ of a baryon can be represented by $(y,\mathbf{p}_t)$. Again, to make the transformation simple, we shall replace $c_t^{\,2}$ in Eq. (2.22) by its expectation value. The corresponding momentum distribution as obtained from Eqs. (2.11) and (2.12) is

$$D^{(0)}(y,\mathbf{p}_t)=\delta(y-y_B)\delta(\mathbf{p}_t)\ , \tag{2.23}$$

and for $n\geq 1$

$$D^{(n)}(y,\mathbf{p}_t)=\frac{\exp[y-y_U(n)]\theta[y_U(n)-y]\theta[y-y_L(n)]}{\{1-\exp[y_L(n)-y_U(n)]\}(n-1)!}\left[-\ln\left[\frac{e^y-e^{y_L(n)}}{e^{y_U(n)}-e^{y_L(n)}}\right]\right]^{(n-1)}\frac{1}{2\pi n\sigma_{tn}^{\,2}}\exp\left[-\frac{p_t^{\,2}}{2\sigma_{tn}^{\,2}}\right], \tag{2.24}$$

where the upper and lower limits $y_U(n)$ and $y_L(n)$ depend on the average of the square of the transverse momentum. They are explicitly given by

$$y_L(n)=y_T+\tfrac{1}{2}\ln(1+2\sigma_{tn}^{\,2}/m^2)\ , \tag{2.25}$$

$$y_U(n)=y_B-\tfrac{1}{2}\ln(1+2\sigma_{tn}^{\,2}/m^2)\ , \tag{2.26}$$

where y_T and y_B are the target and the beam rapidity, respectively, and σ_{tn} depends on the assumption concerning the dependence of the transverse width on the collision number Eq. (2.13) or (2.14).

While the representation of $d\sigma/dx$ by a step function as in Eq. (2.18) is adequate for the region of $x \gg 0$, it may not be realistic in the region of $x \sim 0$ where the phase space opens up slowly after the kinematic constraint is removed. It is reasonable to represent the experimental $pp \to px$ data in a form similar to that of Ref. 15 by

$$\frac{d\sigma}{dx} = A(x - x_L)^{\alpha-1}\theta(1-x)\theta(x-x_L) . \tag{2.27}$$

A properly normalized w function becomes

$$w(\mathbf{p}_{n-1},\mathbf{p}_n) = \alpha \frac{(x_n - x_L)^{\alpha-1}}{(x_{n-1}-x_L)^{\alpha}} \theta(x_{n-1}-x_n)\theta(x_n-x_L) F^{(n)}(\mathbf{p}_{t\,n-1},\mathbf{p}_{tn}) . \tag{2.28}$$

The distribution function is then

$$D^{(n)}(x_n,\mathbf{p}_{tn}) = \alpha^n \left[\frac{x_n-x_L}{1-x_L}\right]^{\alpha-1} \frac{1}{1-x_L} \left[-\ln\left[\frac{x_n-x_L}{1-x_L}\right]\right]^{n-1} \frac{\theta(1-x_n)\theta(x_n-x_L)}{(n-1)!} \frac{1}{2\pi\sigma_{tn}^2} \exp\left[-\frac{p_t^2}{2\sigma_{tn}^2}\right] . \tag{2.29}$$

The x dependence obtained here is similar to, but slightly different from, that obtained in Ref. 31.

In Refs. 15, 30, and 31, for a chain of n collisions, the leading baryon in each of the first $n-1$ collisions suffers energy losses according to the probability function w [Eq. (2.28)] with a stopping-power index α, but the last collision with the stopping-power index changed from α to α'. The parametrization of Eq. (2.28) allows the distribution function $D^{(n)}(x_n,\mathbf{p}_{tn})$ for such a case to be written out explicitly. For completeness, we present the distribution function below:

$$D^{(1)}(x_1,\mathbf{p}_{t1}) = \alpha' \left[\frac{x_1-x_L}{1-x_L}\right]^{\alpha'-1} \frac{1}{1-x_L}\theta(1-x_1)\theta(x_1-x_L)\frac{1}{2\pi\sigma_{tn}^2}\exp\left[-\frac{p_t^2}{2\sigma_t^2}\right] \tag{2.30}$$

and

$$D^{(n)}(x_n,\mathbf{p}_{tn}) = \left[\frac{\alpha^{n-1}\alpha'}{1-x_L}\frac{r_n^{\alpha'-1}-r_n^{\alpha-1}}{(\alpha-\alpha')^{n-1}} - r_n^{\alpha-1}\sum_{k=1}^{n-2}\frac{(-\ln r_n)^k}{k!(\alpha-\alpha')^{n-1-k}}\right]\theta(1-x_n)\theta(x_n-x_L)\frac{1}{2\pi\sigma_{tn}^2}\exp\left[-\frac{p_t^2}{2\sigma_{tn}^2}\right] , \tag{2.31}$$

where

$$r_n = \frac{x_n - x_L}{1-x_L} .$$

These results are the generalizations of those obtained in Refs. 15, 30, and 31. They are useful for purposes of exploring the change of the stopping-power index α as a nucleon transverses the nucleus.[15,30,31] As we shall see, the data of $pA \to px$ at $p = 100$ GeV/c is consistent with $\alpha = \alpha = \alpha' \sim 1.0$, while Refs. 30 and 31 give $\alpha = 3$ and $\alpha' = 1$.

III. pA INELASTIC CROSS SECTIONS

In the multiple-collision model, the probability for the incident nucleon to make a (truly) inelastic collision with a target nucleon is given by the product $T_A(b)\sigma_{\text{in}}$ where $T_A(b)$ is the thickness function of the target nucleus A. In the approximation of small nucleon sizes, the thickness function $T_A(b)$ is given by

$$T_A(\mathbf{b}) = \int \rho_A(\mathbf{b},z)dz , \tag{3.1}$$

where ρ_A is the nucleon density normalized according to

$$\int \rho_A(\mathbf{r})d\mathbf{r} = 1 . \tag{3.2}$$

As a consequence, the thickness function is normalized according to

$$\int T_A(\mathbf{b})d\mathbf{b} = 1 . \tag{3.3}$$

From the probability for the occurrence of n inelastic collisions and the momentum distribution *after* n inelastic collisions $D^{(n)}(x,\mathbf{p}_t)$, the differential cross section for the process $pA \to \text{baryon} \to X$ in an inelastic process is

$$\frac{d\sigma_{\text{in}}^{pA}}{dx\,d\mathbf{p}_t} = \int d\mathbf{b} \sum_{n=1}^{A} \binom{A}{n} D^{(n)}(x,\mathbf{p}_t)[T_A(b)\sigma_{\text{in}}]^n \times [1 - T_A(b)\sigma_{\text{in}}]^{A-n} . \tag{3.4}$$

In the above equation, the subscript "in" denotes an inelastic process which involves at least one inelastic nucleon-nucleon collision. Hence, the summation over n starts at $n = 1$.

We calculate $d\sigma_{\text{in}}^{pA}/dx\,d\mathbf{p}_t$ with the above equation, using a Fermi-type nuclear density distribution with a radius R and a diffuseness a. To compare with the experimental data of $E\,d\sigma/dp^3$ for $pA \to pX$, we assume that in the range of interest, $1 \geq x \geq 0.2$, the fraction of protons among the baryons in the process $pA \to bX$ is independent of A. This is a reasonable assumption as, experimentally, the A dependence of the reaction $pA \to nX$ is the same as the $pA \to pX$ dependence [Fig. 6 of Barton *et al.* (Ref.

25)]. Explicitly, we assume

$$E\frac{d\sigma}{dp^3}(pA\to pX)=cx\frac{d\sigma_{\rm in}^{pA}}{dx\,d\mathbf{p}_t}(pA\to bX)\ , \tag{3.5}$$

where the proton fraction parameter c is determined from the $pp\to pX$ data.

The results of the calculation depend on how the transverse widths depend on the collision number. We shall discuss first the case of an increasing transverse width ($\sigma_{tn}^2=n\sigma_t^2$). We shall use the following set of geometrical parameters:

$$R=1.22A^{1/3}-1.5A^{-1/3}\ \text{fm}\ , \tag{3.6}$$

and $a=0.54$ fm.

We first examine the experimental data of Barton *et al.* for $pA\to pX$ at 100 GeV/c. The $pp\to bX$ data are rather insensitive to the value of α. We use $\alpha=1.05$ for definiteness. The proton fraction parameter c is found to be $c=0.52$. When we compare the theoretical differential cross section $E\,d\sigma/dp^3(pA\to pX)$ with the experimental cross sections of Barton *et al.*,[25] it is found that the experimental cross section of Barton *et al.* at $x\sim0.3$ is higher than the theoretical curves. Varying the geometry parameters of R and a does not improve the results. It appears that the assumption of an increasing transverse width does not agree with the data at 100 GeV/c.

The situation is different for data obtained at a lower energy. We examine the data of Eichten *et al.*[42] at 24 GeV/c in conjunction with the data of Allaby *et al.*[43] at 19 GeV/c. The data $pp\to pX$ at 19 GeV/c requires a proton fraction constant of $c=0.86$. In Fig. 3 the theoretical differential cross section thus obtained is compared with the experimental data at 19 and 24 GeV/c. One finds good agreement between the experimental data points and the theoretical predictions. The agreement indicates that the transverse-momentum width may increase with n for an incident proton momentum around 20 GeV/c but not around 100 GeV/c.

Recently, preliminary experimental data have been obtained from Brookhaven for the reaction $pA\to pX$ at 17 GeV/c. The Brookhaven data[46] differ from the data of Eichten *et al.*[42] and the data of Allaby *et al.*[43] in magnitude and slope. While the questions of absolute normalization and shape are not yet resolved, it is interesting to note that the data of Eichten *et al.* and Allaby *et al.* can be brought to approximate agreement with the Brookhaven data if the latter data are multiplied by a factor of 2.3 (Fig. 3). There is, however, a difference in the shapes around $x\sim0.2$–0.4 which needs to be resolved.

While the data at 100 GeV/c disagree with the model if the transverse width increases with the collision number, we can examine whether the second possibility of a constant transverse-momentum width is consistent with the experimental data. We use again $\alpha=1.05$, the proton fraction parameter of $c=0.52$, and the geometrical parameter of Eq. (3.6). In Fig. 4, the theoretical results are compared with the experimental data of Barton *et al.* The good agreement between the theory and the data suggests that the transverse width at 100 GeV/c does not seem to increase with the collision number. Clearly, the assumption of a constant transverse width is not consistent with the data of Eichten *et al.* and Allaby *et al.* at 24 and 19 GeV/c.

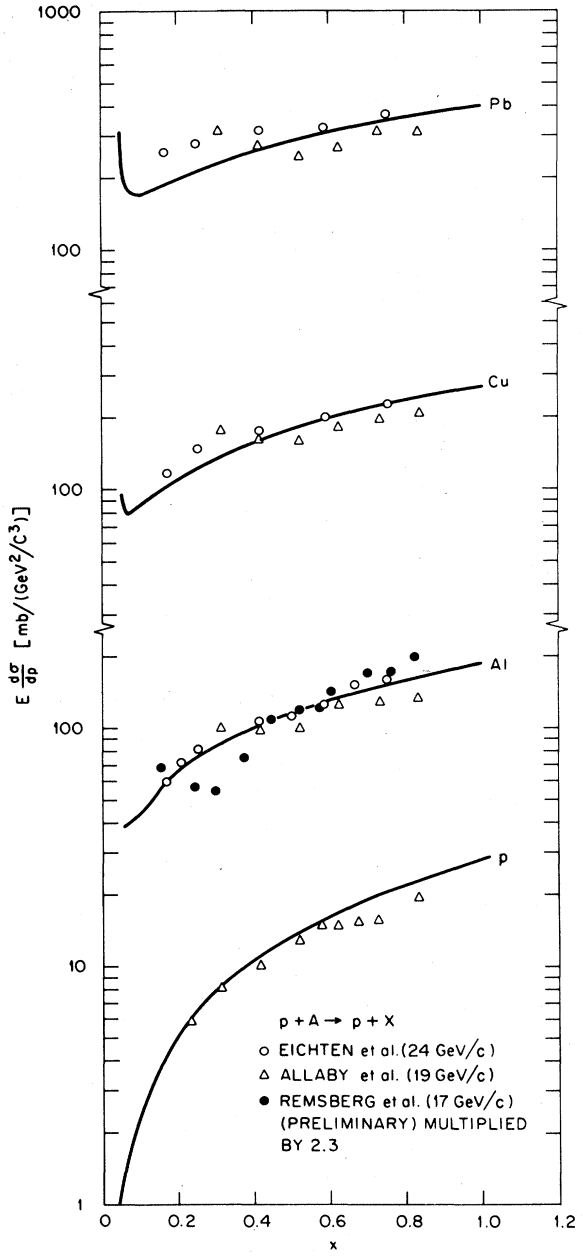

FIG. 3. Comparison of the experimental data for $pA\to pX$ at 19 and 24 GeV/c with the theoretical results obtained under the assumption of a transverse-momentum width increasing with the collision number. Preliminary data points at 17 GeV/c are also shown.

If the data at these energies and the above analysis are correct, there appears to be a change of the mechanism of the scattering process. Around $p_{\rm lab}\sim20$ GeV/c, the transverse-momentum width increases with the collision number as $\sqrt{n}\,\sigma_t$, while for $p\sim100$ GeV/c, it becomes independent of the collision number. If this is indeed the

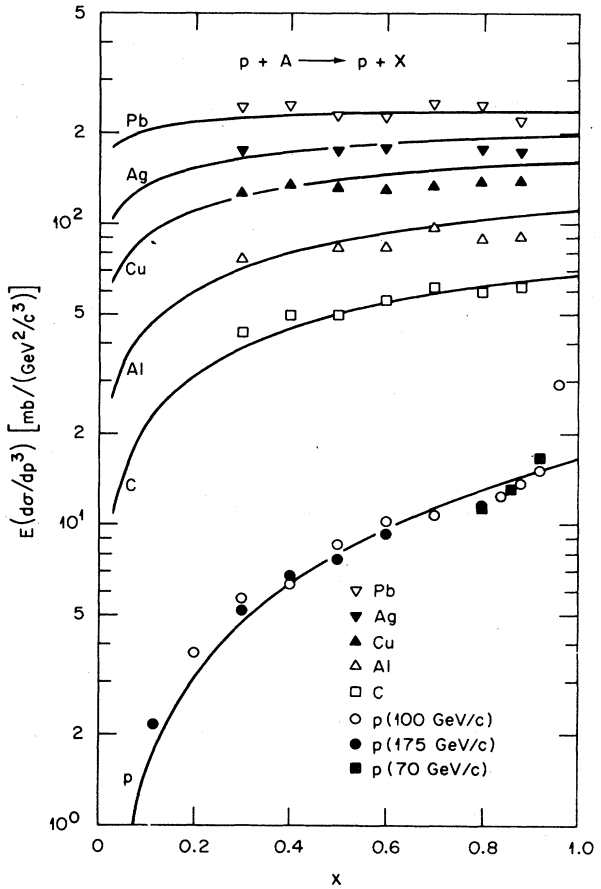

FIG. 4. Comparison of the experimental data for $pA \to pX$ at 100 GeV/c with theoretical results obtained under the assumption of a transverse-momentum width independent of number of collisions.

case, one expects that $\langle p_t \rangle$ of the detected baryons in relativistic heavy-ion collision is greater at 20 GeV/c than it is at 100 GeV/c. It will be of interest to test such a prediction experimentally.

The theoretical calculations we have performed are essentially parameter-free. The radius parameters are not much different from the well-known parameters for nuclear sizes,[47] and the constants λ and c are determined from $pp \to pX$ data. As a further check, we can calculate the total pA inelastic cross section in the multiple-collision-model framework[13]

$$\sigma_{\rm in}^{pA} = \int d\mathbf{b}\{1-[1-T_A(b)\sigma_{\rm in}]^A\} \tag{3.7}$$

and compare this with the pA total absorption cross section σ_a^{pA} which should equal approximately the total inelastic cross section. We find good agreement of $\sigma_{\rm in}^{pA}$ and the experimental data[19] of σ_a^{pA} (Table I). In our previous work,[9,10] the fraction of the quasielastic cross section was not subtracted away from the total inelastic cross section and we used $\lambda=1$, $\sigma_{\rm in}=\sigma_R$. Essentially the same theoretical results of $d\sigma/dx\,d\mathbf{p}_t$ were obtained with $r_0=1.25$ fm and $c=0.53$, but the total inelastic cross sections $\sigma_{\rm in}^{pA}$ were about 10% greater.

In Eq. (3.5) we have assumed that the fraction of protons among the resultant baryons is the same for $pp \to bX$ and $pA \to bX$. This is a good assumption in the range of x around $0.3 \le x \le 1$, as the contribution comes mainly from the incident nucleon having suffered a single collision. When multiple collisions become important, as in the much smaller region of x, it is necessary to take into account the variation of the proton fraction as the number of collisions increases.

TABLE I. Comparison of the theoretical total inelastic cross section $\sigma_{\rm in}^{pA}$ and the experimental total absorption cross section σ_a^{pA} for p-nucleus collisions. The experimental measurements were from Ref. 19. The geometry parameters are given by $R=(1.22A^{1/3}-1.5A^{-1/3})$ fm and $a=0.54$ fm.

Nucleus	σ_a^{pA} (experiment)	$\sigma_{\rm in}^{pA}$ (theory)
H	29.4	29.4
Li	154±5	131.5
Be		165.1
C	222±7	211.2
O		267.3
Al	409±12	402.7
Cu	764±23	756.7
Ag		1113.8
Sn	1179±35	1192.9
Pb	1730±52	1761.0
U		1932.2

IV. STOPPING POWER OF BARYONS IN A NUCLEUS

Although the Feynman scaling variable x and the rapidity variable y can both be used to describe the longitudinal momentum of a particle, the stopping-power equation can best be specified[9,10] in terms of the average value of y instead of the average value of x. With the former, the width of the rapidity distribution behaves as $\sqrt{n-1}$. The average value of y is a reasonable concept when n is not too much greater than unity. For nucleon-nucleus collisions, the greatest average value of n is about 4, and therefore the average value of y is a meaningful concept. On the other hand, in terms of the Feynman scaling variable x, the distribution in x for $n=1$ extends uniformly over the whole range of x, and the average value of x is not as meaningful a concept.

Previously, we obtained the stopping-power equations for a nucleon in nuclear matter in the ultra high-energy limit in which the effects of kinematic constraint and transverse momentum can be neglected.[9] The result is

$$\bar{y}_n = y_B - n\ , \tag{4.1}$$

where $\bar{y}_n$ is the average rapidity of a baryon *after* n collisions and y_B is the beam rapidity. In the presence of the kinematic constraint and the transverse-momentum spreading, the distributions in y and $\mathbf{p}_t$ are given by Eqs. (2.23) and (2.24). The expectation value of $y-y_B$ is

$$\langle y-y_B \rangle = -n - \langle \ln(1-e^{y_L-y}) - \ln(1-e^{y_L-y_B}) \rangle\ . \tag{4.2}$$

For small values of n and $y_B \gg 1$, the last term in Eq.

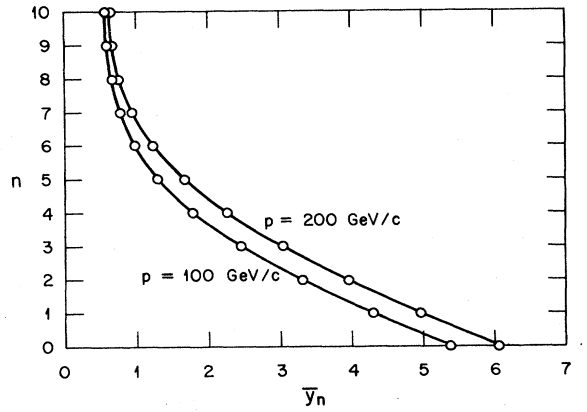

FIG. 5. The dependence of the average value of the rapidity variable $\bar{y}_n$ *after* the nth collision on the collision number n. They are given for two different incident momenta.

(4.2) is negligible, and we obtain the result of Eq. (4.1). As n increases, however, the peak of the rapidity distribution shifts to smaller values of y and the last term cannot be neglected. With the knowledge of the distribution $D^{(n)}(y,\mathbf{p}_t)$ as given by Eqs. (2.23) and (2.24), the expectation value of $y-y_B$ can be obtained numerically. In the numerical work which follows, we shall use the geometrical parameters of $R=1.2A^{1/3}$, $a=0.5234$ fm, and the assumption of increasing transverse width. The other set of parameters and the assumption of fixed transverse width will affect the final results on the produced particles only slightly. We show in Fig. 5 how the average rapidity $\bar{y}_n$ *after* n collisions depends on the collision number n. In line with the usual convention, we put the rapidity axis as the horizontal axis. The calculation was performed for an incident nucleon momentum of 200 and 100 GeV/c, for which the beam rapidities are 6.055 and 5.35, respectively. Initially, the average rapidity decreased approximately by unity for each nucleon-nucleon collision. However, as the nucleon-collision number increases, the average rapidity decreases very slowly.

V. THE RAPIDITY DISTRIBUTION OF PRODUCED PARTICLES

In a highly relativistic nucleus-nucleus collision, the produced particles having rapidities much different from the target or the projectile rapidities are produced outside the nuclei.[21] There are no secondary collisions of these particles with nucleons in the nucleus. Those produced particles having rapidities in the vicinity of the target and projectile rapidities may collide with the target or the projectile nucleons if their spatial coordinates are the same. At high energies, the fraction of these produced particles is, however, quite small, as can be inferred from the rapidity distribution of the produced particles. It is therefore reasonable to neglect the secondary collisions between the produced particles and projectile or target nucleons altogether in the discussion of the rapidity distribution of the produced particles. Particles can also be produced by the collision of recoiling target baryons and other target nucleons. However, the energies of relative motion are small and will only give small contributions to the multiplicity. These collisions can be neglected. Thus, the (initial) rapidity distribution of the produced particles is just an additive supposition of those distributions from all the nucleon-nucleon (or baryon-baryon) collisions. The rapidity distributions thus obtained are only the initial multiplicity distributions before the produced particles interact among themselves. There are situations where the final rapidity distribution may be very close to the initial rapidity distribution. In our case, in the collision of a light projectile the increase in multiplicity may not be great enough for the reaction products to interact strongly among themselves. Even if they interact, if the produced matter follows the law of an ideal fluid without viscosity, it can be shown that the entropy per unit of rapidity is conserved throughout the expansion phase. As the multiplicity is proportional to entropy, the multiplicity distribution per unit rapidity is conserved.[1] If that is the case, the final rapidity distribution is the same as the initial distribution. For these reasons, it is of interest to examine a phenomenological model of particle production where the final rapidity distribution, to be confronted with experimental data, is given by individual nucleon-nucleon collisions in an additive manner without modification.

In the multiple-collision model we have postulated, the probability of collision depends on the thickness function and the baryon-baryon inelastic cross section, and each baryon-baryon collision will produce a number of particles in the same way as a baryon-baryon collision at the same energy in free space. In the collision of a nucleon with a nucleus A at an impact parameter b, the probability of having n inelastic collisions when the nucleon makes an inelastic collision with the target nucleus is[7]

$$P(n,b)=\frac{\binom{A}{n}[T_A(b)\sigma_{\rm in}]^n[1-T_A(b)\sigma_{\rm in}]^{A-n}}{1-[1-T_A(b)\sigma_{\rm in}]^A}\ , \tag{5.1}$$

where the probability is normalized according to

$$\sum_{n=1}^{A}P(n,b)=1\ . \tag{5.2}$$

The rapidity distribution of the produced particles $dN^{pA}(b,y)/dy$ for a collision at impact parameter b is

$$\frac{dN^{pA}}{dy}(b,y) = \sum_{n=1}^{A}P(n,b)\sum_{j=1}^{n}\int dy'd\mathbf{p}_t'D^{(j-1)}(y',\mathbf{p}_t') \times\frac{dN^{(j)}}{dy}\{[s_j(y'p_t')]^{1/2},y\}\ , \tag{5.3}$$

where $dN^{(j)}/dy(\sqrt{s_j},y)$ is the rapidity distribution of the produced particles in the jth baryon-baryon collision for which the center-of-mass energy *before* the jth collision is $\sqrt{s_j}$. The energy $\sqrt{s_j}$ depends on the rapidity and the transverse momentum of the leading baryon $D^{(j-1)}(y',\mathbf{p}_t')$ before the jth collision. To make the results simple, we shall make the approximation that the baryon-baryon rapidity distribution dN/dy needs to be evaluated only at the center-of-mass energy $\sqrt{s_j}$ corresponding to the aver-

age value of y_j and $\mathbf{p}_t^2$. This is a reasonable simplification as the distributions are sharply peaked for small values of j which give the dominant contributions. In this approximation, the kinematic status of the projectilelike baryon is specified by its average values of y and $\mathbf{p}_t^2$. Knowing the rapidity variable and $\mathbf{p}_t^2$, we can then obtain the center-of-mass energy $\sqrt{s_j}$ of the baryon relative to a target nucleon with which it collides. The latter baryon can be taken to be at rest. We obtain then[7]

$$\frac{dN^{pA}}{dy}(b,y)=\sum_{n=1}^{A}P(n,b)\sum_{j=1}^{n}\frac{dN}{dy}(\sqrt{s_j},y)\ , \tag{5.4}$$

where

$$\sqrt{s_j}=\{2m^2+2m[m^2+2(\sigma_{Tj-1})^2]^{1/2}\cosh\bar{y}_{j-1}\}^{1/2}\ , \tag{5.5}$$

and the square of the transverse momentum $\mathbf{p}_t^2$ of the incident baryon has been replaced by its average value of $2(\sigma_{Tj-1})^2$.

In the experiment of Elias *et al.*,[20] there is no impact parameter selection; we need to average Eq. (5.4) over the impact parameter b. For each $\mathbf{b}$, there is a weight of

$$\frac{d\sigma_{\rm in}^{pA}}{d\mathbf{b}}\Big/\sigma_{\rm in}^{pA}\ ,$$

where $d\sigma_{\rm in}^{pA}/d\mathbf{b}$ is

$$\frac{d\sigma_{\rm in}^{pA}}{d\mathbf{b}}=1-[1-T_A(b)\sigma_{\rm in}]^A\ . \tag{5.6}$$

After averaging over the impact parameters, the multiplicity distribution is

$$\left\langle\frac{dN^{pA}}{dy}(y)\right\rangle=\frac{1}{\sigma_{\rm in}^{pA}}\int d\mathbf{b}\sum_{n=1}^{A}\binom{A}{n}[T_A(b)\sigma_{\rm in}]^n[1-T_A(b)\sigma_{\rm in}]^{A-n}\sum_{j=1}^{n}\left[\frac{dN^{(j)}}{dy}(\sqrt{s_j},y)\right]\ . \tag{5.7}$$

Finally, to proceed further, we need to know the nucleon-nucleon dN/dy data as a function of the center-of-mass energy $\sqrt{s_j}$, in the range of energy corresponding to an incident beam momentum of 200 GeV/c and lower. The multiplicity distribution is in the form of a Gaussian function for these energies. We parametrize it so

$$\frac{dN^{(j)}}{dy}(\sqrt{s_j},y)=N(\sqrt{s_j})\frac{1}{\sqrt{2\pi}\,\sigma(\sqrt{s_j})}\exp\left[-\frac{[y-(\bar{y}_{j-1}+y_t)/2]^2}{2[\sigma(\sqrt{s_j})]^2}\right]\ , \tag{5.8}$$

where $N(\sqrt{s_j})$ is the total multiplicity at a center-of-mass energy $\sqrt{s_j}$, $\sigma(\sqrt{s_j})$ is the width of the Gaussian distribution, and y_t is the target rapidity. Experimental data for $N(\sqrt{s_j})$ are given by Eq. (4) of Table II in the tabulation of Albini *et al.*[48]

$$N(\sqrt{s_j})=-0.5+1.27\ln s_j \tag{5.9}$$

which is valid within the range of 3 GeV $\leq\sqrt{s_j}\leq$ 20 GeV. From the data of Elias *et al.*,[20] we can extract

$$\sigma(\sqrt{s_j})=0.585\ln\sqrt{s_j}\ . \tag{5.10}$$

We shall compare the theoretical results from Eq. (5.7) with the experimental pseudorapidity distributions.[20] In such a comparison, it is necessary to convert the rapidity variable y into the pseudorapidity variable defined by

$$\eta=-\ln\left[\tan\frac{\theta_{\rm lab}}{2}\right]\ , \tag{5.11}$$

where $\theta_{\rm lab}$ is the angle of the detected particle relative to the beam direction, measured in the laboratory system. It is easy to show that given y and dN/dy, we can obtain η and $dN/d\eta$ as

$$\eta=\tfrac{1}{2}\ln\frac{(\cosh y)[1-m_c^2/(m_{cT}^2\cosh^2 y)]^{1/2}+\sinh y}{(\cosh y)[1-m_c^2/(m_{cT}^2\cosh^2 y)]^{1/2}-\sinh y}\ , \tag{5.12}$$

and

$$\frac{dN^{pA}}{d\eta}=\left[1-\frac{m_c^2}{m_{cT}^2\cosh^2 y}\right]^{1/2}\frac{dN^{pA}}{dy}\ , \tag{5.13}$$

where m_c and m_{cT} are the rest mass and the transverse mass of the detected particle, respectively. As the produced particles are mostly pions, we can take m_c to be the pion mass. The transverse mass m_{cT} of the pion can be calculated by assuming an average transverse momentum of 0.4 GeV/c as estimated from the $pA\to\pi^+X$ data.[25,49]

With the above equations, the pseudorapidity distribution can be obtained as follows. Given an incident momentum, we first evaluate $\bar{y}_{j-1}$ numerically as in Sec. IV from which the center-of-mass energy $\sqrt{s_j}$ before the jth collision can be obtained from Eq. (5.5). With the knowledge of $\sqrt{s_j}$, the baryon-baryon dN/dy distribution can be calculated from the systematics of Albini *et al.* [Eqs. (5.8)–(5.10)]. Equation (5.7) can be integrated out numerically over b to give the rapidity distribution dN^{pA}/dy averaged over the impact parameters. The rapidity distribution can then be transformed into the pseudorapidity distribution by Eqs. (5.12) and (5.13), to be compared with experimental data. The equations and the numerical calculations are applicable to both the pp collisions and pA collisions.

The systematics of Albini *et al.* give a good description of the $dN^{pp}/d\eta$ data at various incident momenta (Figs. 6, 7, and 8). They are therefore useful for extrapolation to other center-of-mass energies of the colliding baryon along the collision chain. Using the set of parameters $r_0=1.2$ fm, $a=0.5234$ fm, and $\sigma_{\rm in}$ as before, we calculate $\langle dN^{pA}/dy\rangle_b$ from Eq. (5.7) by integrating over b numerically as outlined above. They have been evaluated for the targets of p, ^{12}C, ^{27}Al, ^{63}Cu, ^{108}Ag, ^{208}Pb, and ^{238}U for an incident proton momentum of 200, 100, and 50 GeV/c. With no other free parameters, the theoretical results

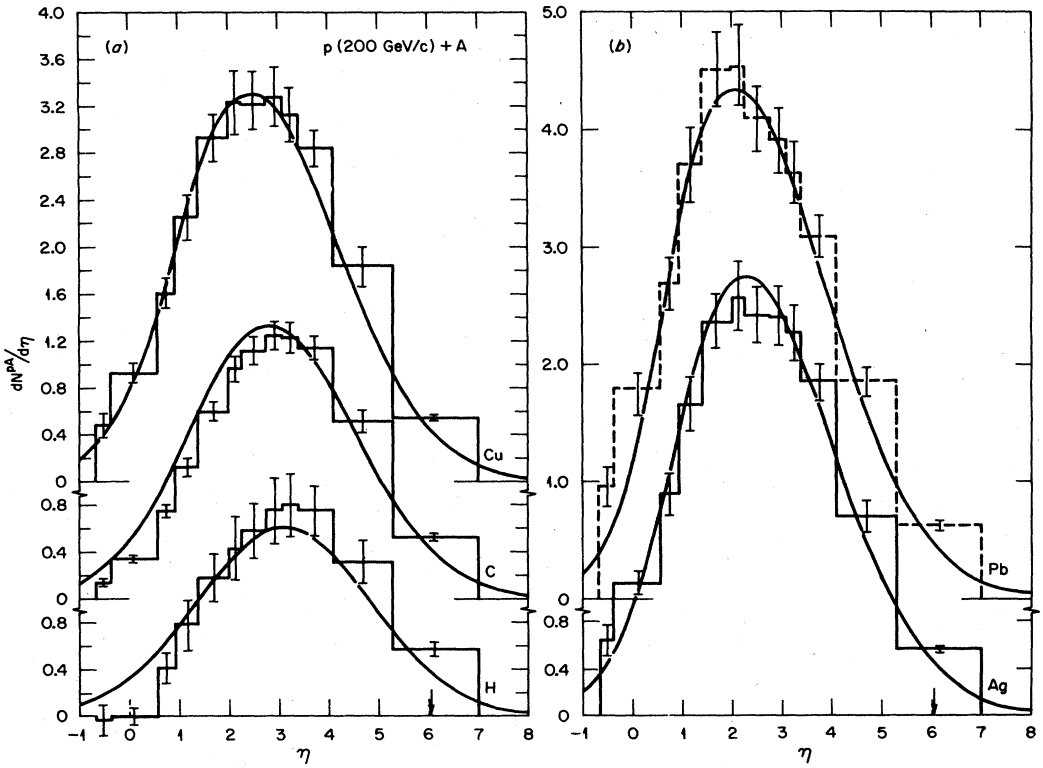

FIG. 6. Comparison of the theoretical results for the total pseudorapidity distribution of produced particles $dN^{pA}/d\eta$ in pA collisions with the experimental data for an incident beam momentum of 200 GeV/c. The solid curves are theoretical results. The histograms are from Ref. 20. To avoid confusion with the histogram for Ag, the histogram for Pb is given by dashed lines. The location of the beam rapidity is indicated by an arrow.

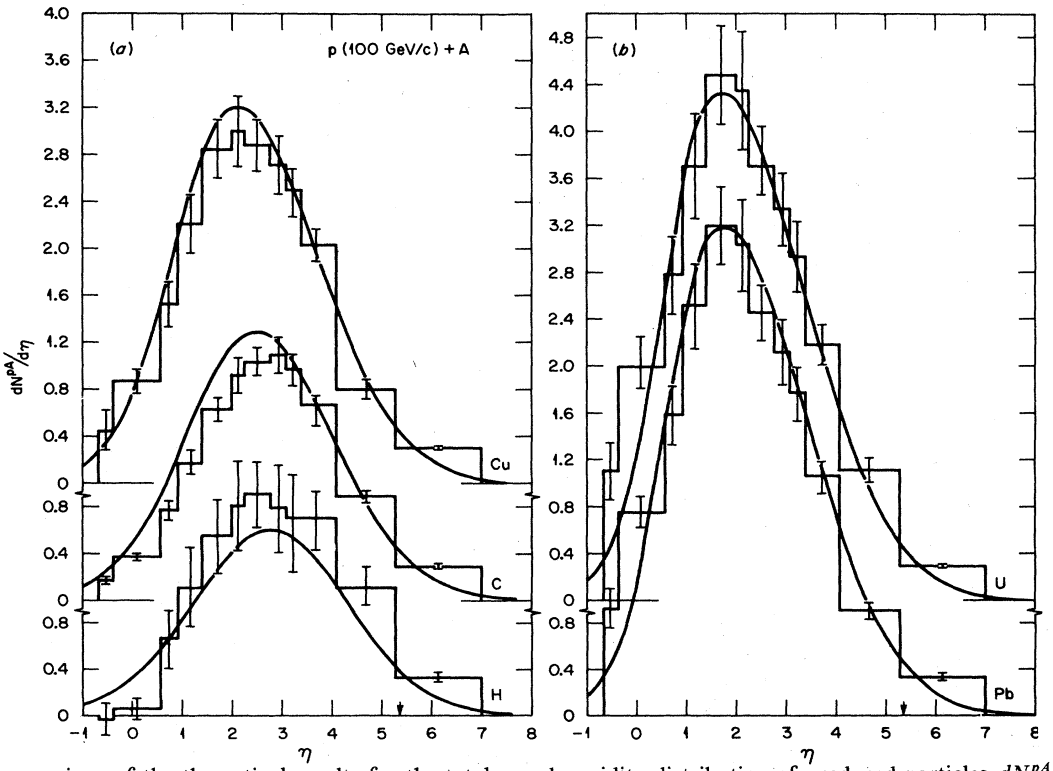

FIG. 7. Comparison of the theoretical results for the total pseudorapidity distribution of produced particles $dN^{pA}/d\eta$ in pA collisions with the experimental data for an incident beam momentum of 100 GeV/c. The solid curves are theoretical results. The histograms are from Ref. 20. The location of the beam rapidity is indicated by an arrow.

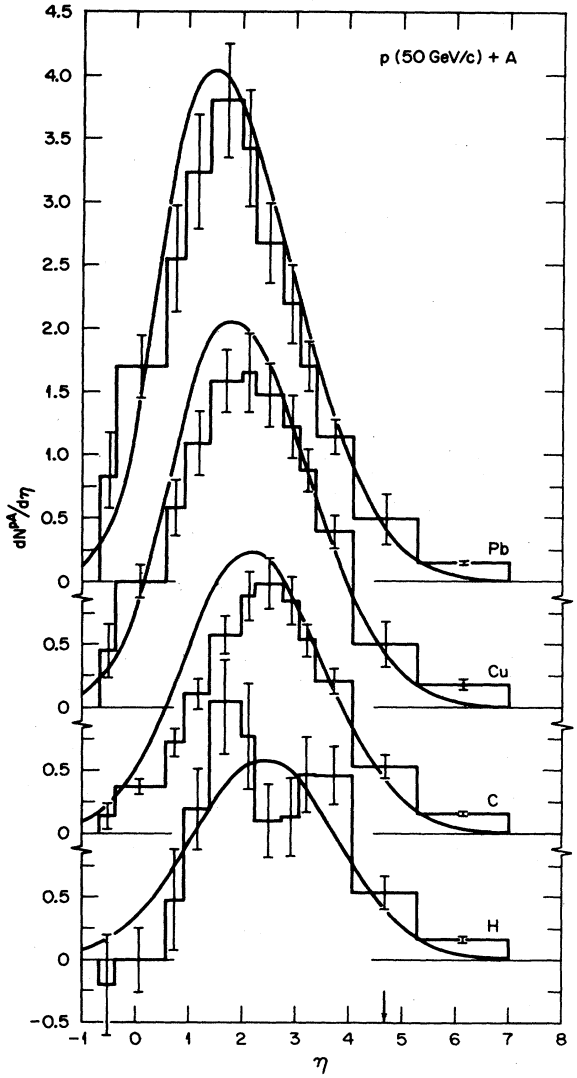

FIG. 8. Comparison of the theoretical results for the total pseudorapidity distribution of produced particles $dN^{pA}/d\eta$ in pA collisions with the experimental data for an incident beam momentum of 50 GeV/c. The solid curves are theoretical results. The histograms are from Ref. 20. The location of the beam rapidity is indicated by an arrow.

agree well with the experimental data (Figs. 6, 7, and 8). The magnitudes and the positions of the peaks are well reproduced. The exceptions are the p-^{12}C results which seem to show a smaller experimental multiplicity in regions $\eta \lesssim 3$. This deviation may be due to the presence of a large oblate deformation for the ^{12}C nucleus, resulting effectively in a more diffused surface with fewer higher-multiple collisions. The agreement for heavy nuclei at 50 GeV/c is not as good as that in the other energies. This may be due to the limitation of the parametrization (5.9) which may give too high a production cross section at low energies near the particle-production threshold.

From the numerical calculations, we see that the ratio R of $\langle dN^{pA}/dy \rangle$ with respect to dN/dy at a rapidity near the beam rapidity is nearly independent of A. With the result of Eq. (5.7), this peculiar feature can be understood by the following reasoning. Particles having a rapidity within half a unit of the beam rapidity must be produced in the first collision of the projectile nucleon with the target nucleons. Subsequent collisions of the resultant baryon can only produce particles with lower rapidities because of the degradation of the energy of the baryon. Thus, for y near y_B, only the term $j=1$ in the summation over j gives any contribution. We have therefore,

$$\frac{dN^{pA}}{dy}(y \sim y_B)$$
$$\cong \frac{1}{\sigma_{\text{in}}^{pA}} \int d\mathbf{b} \sum_{n=1}^{A} \binom{A}{n} [T_A(b)\sigma_{\text{in}}]^n \times [1-T_A(b)\sigma_{\text{in}}]^{A-n} \frac{dN}{dy}(\sqrt{s_1}, y)$$
$$= \frac{dN}{dy}(\sqrt{s_1}, y) . \tag{5.14}$$

Hence, we have in the projectile fragmentation region

$$R(y \sim y_B) \simeq 1$$

as is observed experimentally.[20]

It should be pointed out that while the extrapolation of dN/dy appears to give reasonable results for impact momenta of 200, 100, and 50 GeV/c, the extrapolation of the systematics of Eq. (5.9), valid for 3 GeV $\leq \sqrt{s_{NN}} \leq 20$ GeV, may need to be altered for lower incident energies as the particle-production process has a threshold in $\sqrt{s}$ which is not much greater than $\sqrt{s} \simeq 2$ GeV. In the other extreme, for much higher energies, the distribution dN/dy for nucleon-nucleon collisions is not given by a Gaussian. It is better represented by a Fermi-type distribution whose height and diffuseness depend on the center-of-mass energy. The analysis of pA data at higher energies will require a different extrapolation of the nucleon-nucleon dN/dy data.

VI. PARTICLE PRODUCTION IN THE INCOHERENT-MULTIPLE-COLLISION MODEL

We have analyzed the leading particle (proton) data and the rapidity distribution data in terms of the incoherent-multiple-collision model with some measure of success. There are fragmentation data for nonleading particles such as $\pi^{\pm}$, $K^{\pm}$, $\bar{p}$, etc. In addition, the examination of the signatures of coherent or other peculiar effects in different regions of the rapidity space requires the reference-model results for which the incoherent-multiple-collision model can be quite useful. In this section, we shall derive the expression for the cross section of single nonleading particles in the incoherent-multiple-collision model. The differential cross sections for the nonleading particles have characteristics very different from the leading particle differential cross sections. The spectra of the leading particles are determined by momentum degradation, while those of the nonleading particles come from the hard scattering or fragmentation process. The cross sections are indirectly affected by energy degradation. It is desirable to test further whether our model is also consistent

with the production of nonleading particles in the fragmentation region.

In the multiple-collision model we postulate, particles are produced by baryon-baryon collisions which degrade the momenta of the baryons. With the assumption of no secondary collisions, the production of nonleading particles is just simply superimposed. The probability for the incident baryon with an impact parameter b to make n collisions with the target nucleons N is

$$Q(n,b)=\binom{A}{n}[T_A(b)\sigma_{\text{in}}]^n[1-T_A(b)\sigma_{\text{in}}]^{A-n} \tag{6.1}$$

which is normalized to

$$\sum_{n=0}^{A} Q(n,b)=1 .$$

The differential cross section for the production of a nonleading particle c, in the reaction $pA\to cX$, is given by

$$\frac{d\sigma(pA\to cX)}{dx\,d\mathbf{p}_t}(x,\mathbf{p}_t) = \int d\mathbf{b}\sum_{n=1}^{A} Q(n,b) \times\sum_{j=1}^{n}\int dx'd\mathbf{p}_t' D^{(j-1)}(x'\mathbf{p}_t') \times\frac{dN^{(j)}(bN\to cX)}{dx\,d\mathbf{p}_t}(x'\mathbf{p}_t',x\mathbf{p}_t) . \tag{6.2}$$

The quantity $dN^{(j)}(bN\to cX)/dx\,d\mathbf{p}_t$ is the distribution function after the jth collision for the particle c with momentum $(x,\mathbf{p}_t)$ in a collision of a baryon b of momentum $(x',\mathbf{p}_t')$ on a target nucleon N. In terms of the single-particle cross section, it is given by

$$\frac{dN^{(j)}(bN\to cX)}{dx\,d\mathbf{p}_t}(x',\mathbf{p}_t',x\mathbf{p}_t) = \frac{1}{\sigma_{\text{in}}}\frac{d\sigma^{(j)}(bN\to cX)}{dx\,d\mathbf{p}_t}(x'\mathbf{p}_t',x\mathbf{p}_t) . \tag{6.3}$$

Experimentally, the differential cross sections may depend on the type of incident baryons and on the type of target nucleons. It may be necessary to take this into account. The (baryon)—(target nucleon) cross section should be given by

$$\frac{d\sigma^{(j)}(bN\to cX)}{dx\,d\mathbf{p}_t}=\sum_k \alpha^{(j-1)}(b_k)\frac{d\sigma(b_kN\to cX)}{dx\,d\mathbf{p}_t} , \tag{6.4}$$

where b_k represents a baryon of type k $(p,n,\Delta^{++},\ldots)$ and $\alpha^{(j-1)}(b_k)$ is the fraction of k-type baryons before the jth collision. For the target nucleus, the proton fraction is Z/A and the neutron fraction is N/A. Therefore, the differential cross section $bN\to cX$ for the jth collision is given by

$$\frac{d\sigma^{(j)}(bN\to cX)}{dx\,d\mathbf{p}_t}=\sum_k \alpha^{(j-1)}(b_k)\left[\frac{Z}{A}\frac{d\sigma(b_kp\to cX)}{dx\,d\mathbf{p}_t}+\frac{N}{A}\frac{d\sigma(b_kn\to cX)}{dx\,d\mathbf{p}_t}\right] . \tag{6.5}$$

Combining all these results together, we obtain the general expression for the single-particle cross section in the incoherent-multiple-collision model,

$$\frac{d\sigma(pA\to cX)}{dx\,d\mathbf{p}_t}(x,\mathbf{p}_t) = \int\frac{d\mathbf{b}}{\sigma_{\text{in}}}\sum_{n=1}^{A} Q(n,b)\sum_{j=1}^{n}\int dx'd\mathbf{p}_t' D^{(j-1)}(x'\mathbf{p}_t')\sum_k \alpha^{(j-1)}(b_k)\left[\frac{Z}{A}\frac{d\sigma(b_k\to cx)}{dx\,d\mathbf{p}_t}+\frac{N}{A}\frac{d\sigma(b_kn\to cx)}{dx\,d\mathbf{p}_t}\right] . \tag{6.6}$$

VII. FRAGMENTATION CROSS SECTION FOR $pA\to\pi^{\pm}X$

From the results of Eq. (6.6), we see that a complete analysis of the fragmentation data in the $pA\to cX$ reactions requires the knowledge of the baryon fraction after a baryon-baryon collision and the experimental cross sections. In general, the baryon fraction $\alpha^{(j)}$ evolves according to

$$\alpha^{(j)}(b_k)=\sum M_{kl}\alpha^{(j-1)}(b_l) , \tag{7.1}$$

where the branching matrix element M_{kl} for an incident l-type baryon branching into a k-type leading baryon needs to come from experimental data. We know only the proton fraction $M_{pp}=\alpha_0$ after a pp collision, while the fractions for the other baryons are not known.

Experimental $d\sigma/dx$ data[50] for $pp\to px$ and $pn\to pX$ (backward) at 19 GeV/c indicate that at that energy the proton and neutron fractions exhaust nearly all the baryon fractions in a pp collision. Furthermore, in the region of $x\gtrsim 0.3$, the produced particles come essentially from the first of the chain of collisions. (Our numerical calculations confirm that this is indeed the case.) It is therefore safe to approximate the small contributions from the subsequent collisions by taking only the proton and the neutron as the resultant baryon in the collision chain. For an incident proton [i.e., $\alpha^{(0)}(p)=1$ and $\alpha^{(0)}(n)=0$], the proton fraction after an inelastic scattering is $\alpha^{(1)}(p)\equiv\alpha_0=0.52$ (Sec. III). Therefore, after j collisions, the proton fraction is

$$\alpha^{(j)}(p)=\sum_{\substack{i=0\\ i=\text{even}}}^{j}\binom{j}{i}\alpha_0{}^{j-i}(1-\alpha_0)^i \tag{7.2}$$

and the neutron fraction is

$$\alpha^{(j)}(n)=\sum_{\substack{i=1\\ i=\text{odd}}}^{j}\binom{j}{i}\alpha_0{}^{j-i}(1-\alpha_0)^i\ . \tag{7.3}$$

The fractions of proton and neutron approach one-half rapidly as j increases.

To proceed further, it is necessary to know the cross sections for different fragmentation reactions. In what follows, to avoid confusion with respect to the projectile or the target fragmentation regions, we shall adopt the notation that $PT\to cX$ denotes the reaction of an incident projectile P on a target T producing particle c in the *projectile* fragmentation region. While the experimental data for $pp\to cX$ are quite extensive, those for $pn\to cX$ are less so, and the data for $np\to cX$ and $nn\to cX$ are very scarce. In the projectile fragmentation region, we expect the cross sections to be independent of the target

$$d\sigma(pp\to cX)\cong d\sigma(pn\to cX)$$

and (7.4)

$$d\sigma(np\to cX)\cong d\sigma(nn\to cX)\ .$$

Comparison of the $pp\to\pi^-X$ data[25,51] and $pn\to\pi^-X$ data[52] at 100–200 GeV/c shows that indeed[53,54]

$$\frac{d\sigma}{dx}(pp\to\pi^-X)\cong\frac{d\sigma}{dx}(pn\to\pi^-X)\ . \tag{7.5}$$

Comparison of $pp\to\pi^+X$ data[25,51] and $pn\to\pi^+X$ data[52] shows that the cross sections are about the same for $x<0.3$, but for $x>0.3$ $d\sigma(pn\to\pi^+X)$ is greater than $d\sigma(pp\to\pi^+X)$ by above a factor of 2. These differences call for further experimental measurements in the region of large x as there are "difficulties in momentum resolution. . .of very-high-energy particles."[52] Until these differences are resolved, we shall assume that the projectile fragmentation cross section is independent of the target [i.e., Eq. (7.4)].

We shall discuss only pion production in the remainder of this section. Because of isospin symmetry, the cross sections for $np\to\pi^\pm x$ and $nn\to\pi^\pm x$ are related to those for pn and pp by

$$d\sigma(np\to\pi^\pm X)=d\sigma(pn\to\pi^\mp X) \tag{7.6}$$

and

$$d\sigma(nn\to\pi^\pm X)=d\sigma(pp\to\pi^\mp X)\ . \tag{7.7}$$

The baryon-nucleon$\to\pi^\pm X$ cross section of Eq. (6.4) can be written in terms of $pp\to\pi^\pm X$ cross sections

$$\frac{d\sigma(bN\to\pi^\pm X)}{dx\,d\mathbf{p}_t}=\alpha^{(j-1)}(p)\frac{d\sigma(pp\to\pi^\pm X)}{dx\,d\mathbf{p}_t}+\alpha^{(j-1)}(n)\frac{d\sigma(pp\to\pi^\mp X)}{dx\,d\mathbf{p}_t}\ . \tag{7.8}$$

The experimental differential cross section for the reaction $pp\to cX$ can be represented by[26]

$$\frac{d\sigma(pp\to cX)}{dx\,d\mathbf{p}_t}=\frac{1}{x}C(c,p_t)(1-x)^{\eta(c)}\ . \tag{7.9}$$

We can parametrize C as a Gaussian function in $\mathbf{p}_t$ with the same standard deviation as that for $pp\to px$,

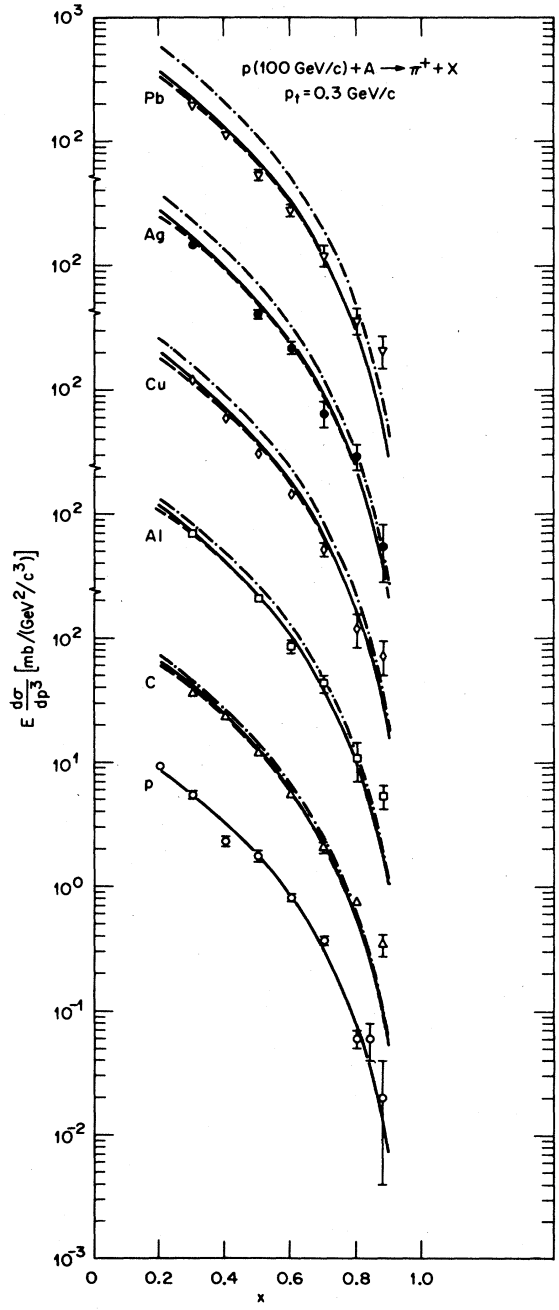

FIG. 9. Comparison of the theoretical and the experimental single-particle inclusive fragmentation cross section for $pA\to\pi^+X$ at an incident momentum of 100 GeV/c and $p_t=0.3$ GeV/c. The solid curves are the theoretical results with a reduction parameter $\kappa=0.15$. They include contributions from all collisions. The dashed curves are results from the first-collision approximation [Eq. (8.3)] with $\kappa=0.15$. The dashed-dot curves are theoretical results with no reduction parameter.

$$C(c,p_t)=\frac{A(c)}{2\pi\sigma_t^{\,2}}\exp\left[-\frac{p_t^{\,2}}{2\sigma_t^{\,2}}\right], \tag{7.10}$$

where $A(c)$ can be obtained from the tabulated values[26] of $C(c,p_t)$. The cross section $pA\to\pi^{\pm}X$ of Eq. (6.6) can be finally written as

$$\frac{d\sigma(pA\to\pi^{\pm}X)}{dx\,d\mathbf{p}_t}=\int\frac{d\mathbf{b}}{\sigma_{\rm in}}\sum_{n=1}^{A}Q(n,b)\sum_{j=1}^{n}[\alpha^{(j-1)}(p)\mathscr{D}_{+}^{(j)}(x,\mathbf{p}_t)+\alpha^{(j-1)}(n)\mathscr{D}_{-}^{(j)}(x,\mathbf{p}_t)], \tag{7.11}$$

where the distributions $\mathscr{D}_{\pm}^{(j)}$ are given by

$$\mathscr{D}_{\pm}^{(j)}(x,\mathbf{p}_t)=\frac{A(\pi^{\pm})}{(\sigma_{tj})^2}\exp\left[-\frac{p_t^{\,2}}{(\sigma_{tj})^2}\right]\times\int_x^1 dx'\frac{x'}{x}\left[1-\frac{x}{x'}\right]^{\eta(\pi^{\pm})}\times\left[-\ln\left[\frac{x'-x_L}{1-x_L}\right]\right]^{j-2}\frac{1}{(j-2)!}, \tag{7.12}$$

and $x_L=x_L(j-1)$ is defined by Eq. (2.13).

In this simple theory, the input parameters are the experimental nucleon-nucleon cross sections as parametrized by $C(\pi^{\pm})$ and $\eta(\pi^{\pm})$, the proton fractions α_0 having been determined previously ($\alpha_0=0.52$). We can find the parameters of $C(\pi^{\pm})$ and $\eta(\pi^{\pm})$ from Table 16 of Brenner *et al.*[26] For $p_t=0.3$ GeV/c and an incident momentum of 100 GeV/c, we have[26]

$$\begin{aligned}&C(\pi^+)\equiv C(pp\to\pi^+X)\\&\quad=18.09\ \text{mb}/(\text{GeV}^2/c^3),\\&\eta(\pi^+)\equiv\eta(pp\to\pi^+X)=3.39,\\&C(\pi^-)\equiv C(pp\to\pi^-X)\\&\quad=12.17\ \text{mb}/(\text{GeV}^2/c^3),\end{aligned} \tag{7.13}$$

and

$$\eta(\pi^-)\equiv\eta(pp\to\pi^-X)=4.39\ .$$

Using this set of parameters of $C(\pi^{\pm})$ and $\eta(\pi^{\pm})$, as determined from previous measurements, we calculate the differential cross section for the reaction $pA\to\pi^+X$ with Eqs. (7.11) and (7.12) and the same geometrical parameters of r_0, a, and $\sigma_{\rm in}$ as before. The integrations in these equations are carried out numerically. The theoretical results thus obtained are shown as the dashed-dot curves in Fig. 9 and compared with the experimental data of Barton *et al.*[25] One finds that the incoherent-multiple-collision model gives the correct shapes of the cross sections, but the magnitudes are systematically greater than the experimental results. The heavier the projectile, the greater are the deviations.

It is difficult at this stage to pinpoint precisely the origin of the coherent effect which can produce such a deviation. A plausible explanation is the interference of subsequent collisions on the production of energetic particles. One can infer from the inside-outside-cascade picture that in the laboratory frame, the more energetic the produced particle, the later it is produced.[40] But the late production is likely to occur at the same time when the incident baryon is making subsequent collision with nucleons along the chain. These subsequent collisions probably reduce the production of energetic particles, although they may have little effect on the production of slower particles produced earlier. To account for such an effect, we introduce a phenomenological reduction factor for the jth collision along a chain of m collisions. Clearly, the physical quantity concerning subsequent collisions is its number $(n-j)$ and the simplest factor one can write down is a linear form $1-(n-j)\kappa$, with κ the reduction parameter. To specify the reduction of the production of energetic particles at the jth collision due to the presence of subsequent $n-j$ collisions in a chain of n collisions, we modify Eq. (6.6) to include the reduction factor as

$$\frac{d\sigma(pA\to cX)}{dx\,d\mathbf{p}_t}(x,\mathbf{p}_t)=\int\frac{d\mathbf{b}}{\sigma_{\rm in}}\sum_{n=1}^{A}Q(n,b)\sum_{j=1}^{n}[1-(n-j)\kappa]\theta[1-(n-j)\kappa]\times\int dx'd\mathbf{p}_t'D^{(j-1)}(x'\mathbf{p}_t')\sum_k\alpha^{(j-1)}(b_k)\frac{d\sigma(b_kN\to cX)}{dx\,d\mathbf{p}_t}(x'\mathbf{p}_t',x\mathbf{p}_t), \tag{7.14}$$

where the step function is to ensure that the contributions are positive definite.

With this phenomenological reduction factor, a value of $\kappa=0.15$ gives the cross sections for $pA\to\pi^+X$ at $p_t=0.3$ GeV/c as solid curves (Fig. 9). There is a good agreement between the theoretical results and the experimental data points for all the nuclei of C, Al, Cu, Ag, and Pb under consideration.

The reduction factor may be a useful phenomenological concept if the same parameter can also explain the other data of $pA\to\pi^-X$, $pA\to K^+X$, and $pA\to\bar{p}X$. We calculate cross sections for $pA\to\pi^-X$ with the same reduction factor of $\kappa=0.15$. The results are shown as the solid curves in Fig. 10. It is gratifying that there is again a good agreement with the experimental data when the incoherent-multiple-collision model is modified in the same way.

We can examine the contributions of higher multiple collisions to the production of $\pi^{\pm}$ in this range of $x>0.2$. We show in Figs. 8 and 9 the cross sections of $pA\to\pi^{\pm}X$ coming from only the first collision of the incident projectile nucleon as the dashed curves. Clearly, the contributions from higher multiple collisions are very small for light target masses and large values of x. For pPb$\to\pi^{\pm}X$ at $x=0.2$, the contributions from the first collision are about 90% of the total.

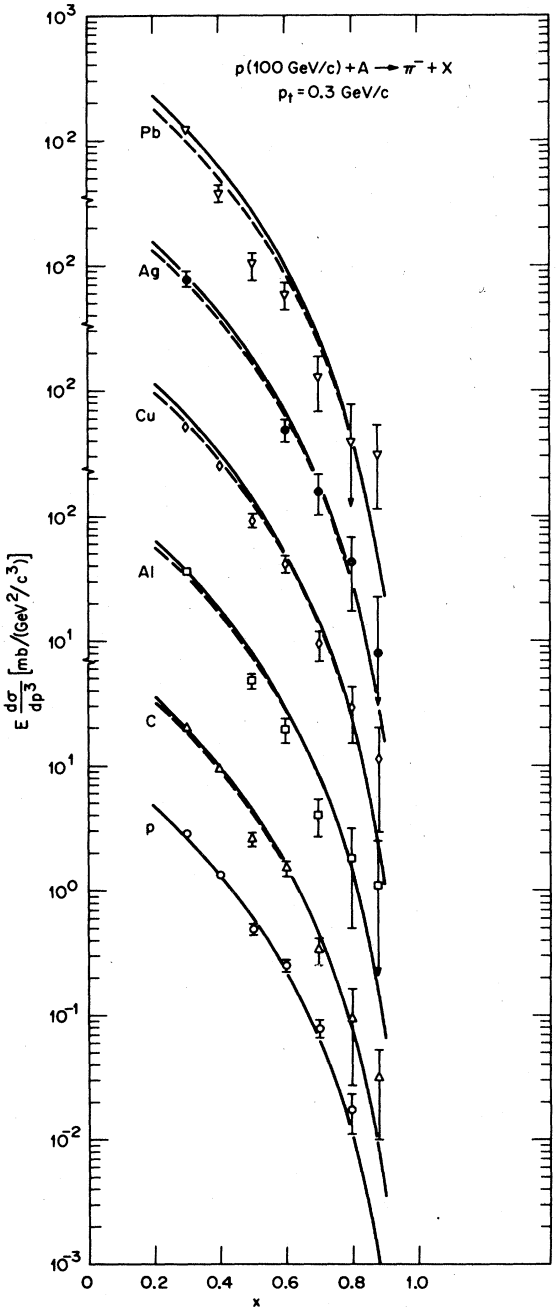

FIG. 10. Comparison of the theoretical and the experimental cross sections for $pA \to \pi^- X$ at an incident momentum of 100 GeV/c and $p_t = 0.3$ GeV/c. The solid curves are theoretical results from our model with a reduction parameter $\kappa = 0.15$ and include contributions from all collisions. The dashed curves are results from the first-collision approximation [Eq. (8.3)] with $\kappa = 0.15$.

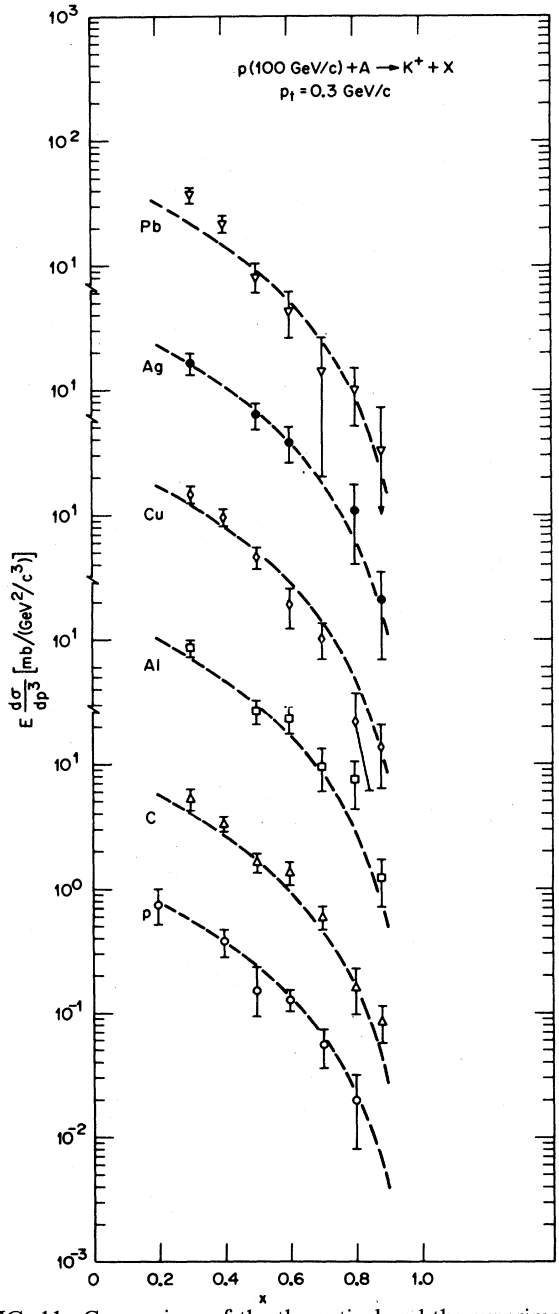

FIG. 11. Comparison of the theoretical and the experimental cross sections for $pA \to K^+ X$ at an incident momentum of 100 GeV/c and $p_t = 0.3$ GeV/c. The theoretical results are obtained with the first-collision approximation [Eq. (8.3)] with $\kappa = 0.15$.

VIII. FIRST-COLLISION APPROXIMATION FOR THE $pA \to cX$ FRAGMENTATION CROSS SECTION

The results of the last section allow us to examine qualitatively the mass-number dependence of the inclusive fragmentation cross section (for nonleading particles). As we mentioned before, even though the incident proton can make many collisions with the target nucleons, essentially only the first inelastic collision can produce energetic particles in the fragmentation region of $x \gtrsim 0.3$. Subsequent collisions of the incident baryon produce particles with smaller values of x. This means mathematically that the produced particles come essentially from the $j = 1$ term in the sum over j in Eq. (6.2). If we neglect the other smaller contributions from $j > 1$, we get from Eq. (7.14) the approximation

$$\frac{d\sigma(pA\to cX)}{dx d\mathbf{p}_t}(x,\mathbf{p}_t)\sim \int d\mathbf{b}\sum_{n=1}^{A} Q(n,b)[1-(n-1)\kappa]\frac{1}{\sigma_{\rm in}}\frac{d\sigma(pN\to cX)}{dx\, d\mathbf{p}_t}(x,\mathbf{p}_t). \tag{8.1}$$

We recognize the definition of pA inelastic cross sections,

$$\sigma_{\rm in}^{pA}=\int d\mathbf{b}\sum_{n=1}^{A} Q(n,b)$$
$$=\int d\mathbf{b}\{1-[1-T_A(b)\sigma_{\rm in}]^A\}\ . \tag{8.2}$$

Therefore, we have

$$\frac{d\sigma(pA\to cX)}{dx\, d\mathbf{p}_t}\cong\frac{\sigma_{\rm in}^{pA}}{\sigma_{\rm in}}[1-(\nu-1)\kappa]\frac{d\sigma(pp\to cX)}{dx\, d\mathbf{p}_t}$$
$$=\frac{A}{\nu}[1-(\nu-1)\kappa]\frac{d\sigma(pp\to cX)}{dx\, d\mathbf{p}_t}\ , \tag{8.3}$$

where ν is the average number of collisions

$$\nu=\frac{A\sigma_{\rm in}}{\sigma_{\rm in}^{pA}}\ . \tag{8.4}$$

As $\sigma_{\rm in}^{pA}$ is approximately proportional to $A^{2/3}$, the fragmentation cross section for $pA\to cX$ is approximately proportional to $A^{2/3}$, in agreement with experiment.[25]

To analyze the kaon production data, we note that we do not have sufficient data to follow the collision chain. Although experimental data for $pp\to K^{\pm}X$ is available, those for (pn, np, and nn)$\to K^{\pm}X$ are not. As the first collision is the dominant component of the collision chain, we shall analyze $pA\to K^{\pm}X$ data using the first-collision approximation of Eq. (8.3) and the numerically integrated cross section $\sigma_{\rm in}^{pA}$ (Table I).

In applying Eq. (8.3) to analyze $pA\to K^{\pm}X$ data, we find it convenient to parametrize the $pp\to K^{\pm}X$ data in the form of Eq. (7.9). The parameters at 100 GeV/c and $p_t=0.3$ GeV/c for $pp\to K^{+}X$ are[26]

$$C(K^{+})=1.41\ \text{mb}/(\text{GeV}^2/c^3)$$

and (8.5)

$$\eta(K^{+})=2.56\ ,$$

and for $pp\to K^{-}X$ are

$$C(K^{-})=0.92\ \text{mb}/(\text{GeV}^2/c^3)$$

and (8.6)

$$\eta(K^{-})=4.59\ .$$

With the reduction parameter $\kappa=0.15$ determined previously from $pA\to\pi^{+}X$ data, we obtain cross sections for the reactions $pA\to K^{\pm}X$. The theoretical results are shown as the dashed curves in Figs. 11 and 12. It is gratifying that the experimental data agree well with the theoretical predictions without additional parameters.

Barton *et al.*[25] also give data for the reaction $pA\to\bar{p}X$. The $pp\to\bar{p}X$ data are too scanty to be used as the basic cross section to generate the cross sections for the other nuclei. Instead, we parametrize the pCu$\to\bar{p}X$ data. At $p_t=0.3$ GeV/c, they are given by

$$x\frac{d\sigma}{dx\, d\mathbf{p}_t}=12.75(1-x)^6\text{mb}/(\text{GeV}/c)^2\ .$$

From the experimental data for Cu, we calculate $pA\to\bar{p}X$ cross sections for the other nuclei with Eq. (7.3) using the same reduction parameter $\kappa=0.15$ as before. There is a good agreement between the predictions and experiment

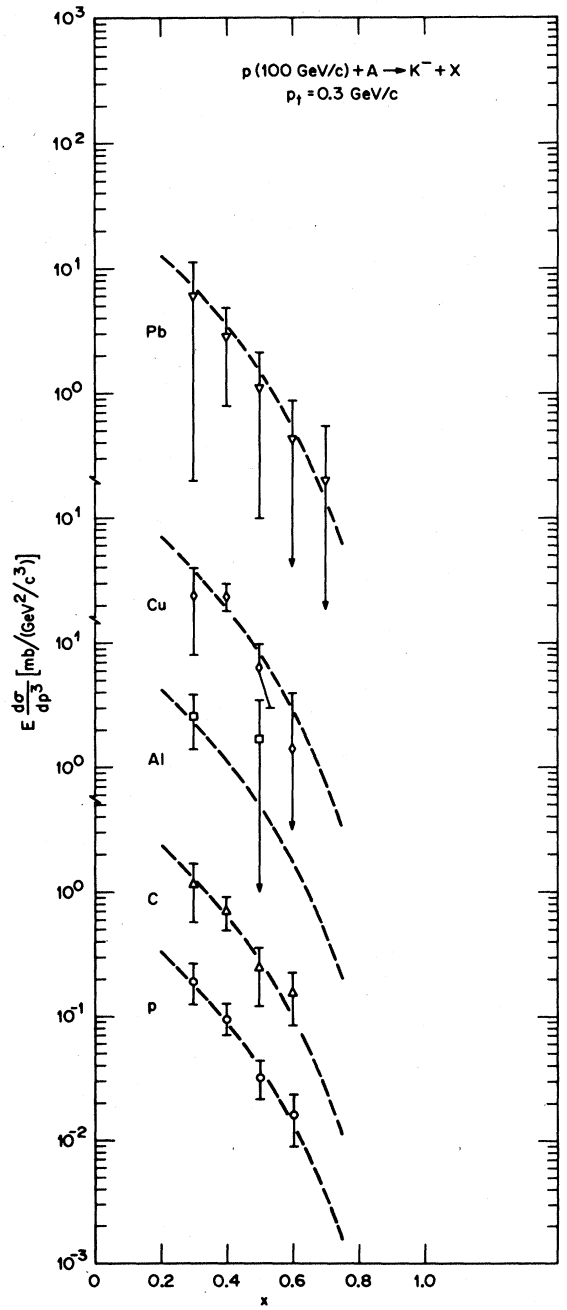

FIG. 12. Comparison of the theoretical and the experimental cross sections for $pA\to K^{-}X$ at an incident momentum of 100 GeV/c and $p_t=0.3$ GeV/c. The theoretical results are obtained with the first-collision approximation [Eq. (8.3)] with $\kappa=0.15$.

(Fig. 13). The experimental statistical errors are, however, quite large.

IX. MODIFIED MULTIPLE-COLLISION MODEL

The results we have obtained in the last few sections indicate that the incoherent-multiple-collision model can explain the rapidity density dN^{pA}/dy in the central rapidity region with no parameters, but needs simple modification and a single parameter for the data of $pA \to \pi^+ X$, $pA \to \pi^- X$, $pA \to K^+ X$, $pA \to K^- X$, and $pA \to \bar{p} X$ in the fragmentation region. Although both the dN^{pA}/dy data and the fragmentation data appear to be equally important, it is necessary to realize that the central rapidity dN^{pA}/dy data are the bulk part of the rapidity density distribution. Our comparison indicates that the model may be a good first approximation which nevertheless needs finer modifications for the tail part of the distributions.

With the model modified for the fragmentation region, it is of interest to seek a unified description throughout the whole rapidity space. The parameter κ is 0.15 in the fragmentation region but is apparently zero in the central rapidity region. A unified description calls for a reduction factor which depends on rapidity. This is a reasonable concept as the production of slow particles (in the laboratory system) occurs before the incident baryon collides with the next target nucleon. To be consistent with the fragmentation data, it is necessary to modify Eq. (5.7) for produced particles to include a reduction factor $\kappa(y)$ which depends on rapidity

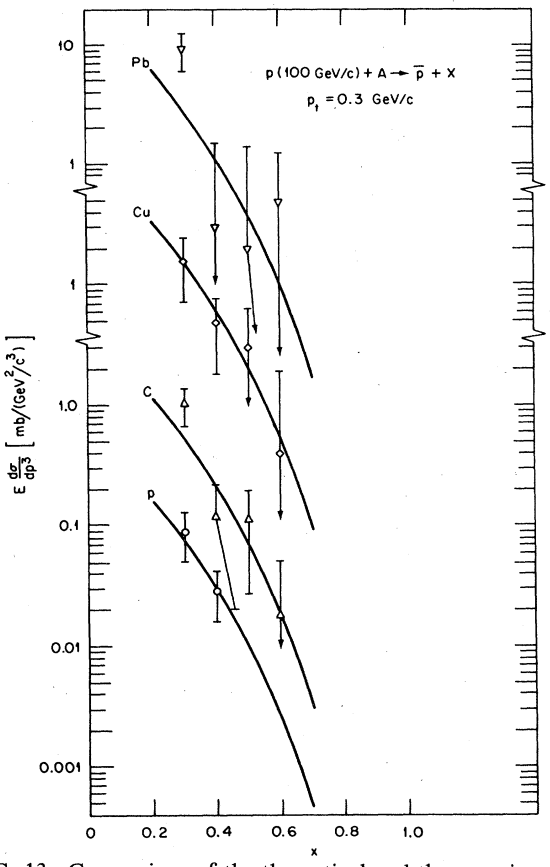

FIG. 13. Comparison of the theoretical and the experimental cross sections for $pA \to \bar{p} X$ at an incident momentum of 100 GeV/c and $p_t = 0.3$ GeV/c. The theoretical results are obtained with the first-collision approximation [Eq. (8.3)] with $\kappa = 0.15$.

$$\left\langle \frac{dN^{pA}}{dy}(y) \right\rangle = \int \frac{d\mathbf{b}}{\sigma_{\text{in}}^{pA}} \sum_{n=1}^{A} Q(n,b) \sum_{j=1}^{n} [1-(n-j)\kappa(y)]\theta[1-(n-j)\kappa(y)] \frac{dN^{(j)}}{dy}(\sqrt{s_j}, y) , \tag{9.1}$$

where

$$\kappa(y) \to 0.15 \quad \text{for} \quad \left| y - \frac{\bar{y}_{j-1} + y_t}{2} \right| \gtrsim y_c$$

and

$$\kappa(y) \to 0 \quad \text{for} \quad \left| y - \frac{\bar{y}_{j-1} + y_t}{2} \right| \lesssim y_c .$$

The crossover rapidity y_c is as yet not well determined but is probably about 1—1.5 units of rapidity less than the beam rapidity.[55] Clearly, such a modification only alters the tail part of the rapidity density and will preserve the good agreement of the rapidity density in the central rapidity region. In a similar manner, the single-particle-production cross section for the reaction $pA \to cX$ in the modified multiple-collision model is given by

$$\frac{d\sigma(pA \to cX)}{dy\, d\mathbf{p}_t}(x, \mathbf{p}_t)$$

$$= \int \frac{d\mathbf{b}}{\sigma_{\text{in}}} \sum_{n=1}^{A} Q(n,b) \sum_{j=1}^{n} [1-\kappa(y)(n-j)]\theta[1-\kappa(y)(n-j)]$$

$$\times \int dx'\, d\mathbf{p}_t'\, D^{(j-1)}(x', \mathbf{p}_t') \sum_k \alpha^{(j-1)}(b_k) \left[\frac{Z}{A} \frac{d\sigma(b_k p \to cX)}{dy\, d\mathbf{p}_t} + \frac{N}{A} \frac{d\sigma(b_k n \to cX)}{dy\, d\mathbf{p}_t} \right] .$$

X. SUMMARY AND DISCUSSION

We undertake to examine the incoherent-multiple-collision model by comparing its predictions with experimental data. In this model, baryon-baryon collisions produce particles and degrade the baryon momenta in the same way as nucleon-nucleon collisions in free space, the probability of the collision being given by the thickness function and the nucleon-nucleon inelastic cross section. It is further assumed that there are no secondary collisions of the produced particles with the target or projectile nucleons. The basic process in this model is the baryon-baryon collision from which all other data are derived. When the experimental baryon-baryon data are available, the theory is parameter-free and provides a "benchmark" comparison whereby peculiarities due to coherent effects may show up as systematic deviations.

We compare the predictions of the model with an extensive set of experimental data. We study $pA \to pX$ to examine the spectra of the leading particles and their dependence on the mass number A. We investigate the rapidity distributions for nucleon-nucleus collisions as a function of bombarding momenta and target-mass number for the whole range of rapidity. We also study the production of nonleading particles $\pi^{\pm}$, $K^{\pm}$, and $\bar{p}$ in the fragmentation region. The cross sections of the $pA \to pX$ reaction and the pseudorapidity distribution $dN^{pA}/d\eta$ are well reproduced. Other qualitative features such as the approximate unity of the ratio

$$R = (dN^{pA}/dy)/(dN^{pp}/dy)$$

near the beam rapidity also emerge naturally in the model. These results lend support to the approximate description of the nucleon-nucleus collision as a succession of incoherent elementary baryon-baryon collisions, with perhaps small modifications. They also provide the justification for a multiple-collision description of a nucleus-nucleus collision for the rapidity density in the central rapidity region which forms the basis[7] for a previous estimate of the initial energy density of the quark-gluon plasma in highly relativistic heavy-ion collisions.

While the agreement between the theory and the experiment is substantive, there are also some experimental data which are peculiar and appear to be deviations from other similar data and from the model. It is important to repeat these measurements or perform similar measurements in order to confirm or exclude these peculiar pieces of data from our consideration. Of particular interest is the $pA \to pX$ data for small values of x and heavy nuclei where the data of Eichten *et al.*[42] and Allaby *et al.*[43] appear to give a cross section different from the data of Barton *et al.*[25] If the cross-section data are all correct, it may be an indication of a change of the proton-production mechanism as energy increases.

In the fragmentation region, however, the incoherent-multiple-collision model predicts too large a cross section for nonleading particles. As the most energetic particles are produced last, they are affected by the presence of subsequent collisions. By allowing a phenomenological reduction factor as depending on the number of subsequent collisions, a modified multiple-collision model gives predictions of the cross section of $pA \to \pi^+X$, $pA \to \pi^-X$, $pA \to K^+X$, $pA \to K^-X$, and $pA \to \bar{p}X$ in good agreement with experiment.

The phenomenological reduction factor is introduced in the linear form of $1-(n-j)\kappa$ which could well be in other forms such as $(1-\kappa)^{n-j}$ or $e^{-\kappa(n-j)}$ having the same terms linear in κ. The latter two forms have the appearance of an attenuation factor. The origin of the reduction factor suggests that the value of κ is likely to depend on the incident energy. As energy decreases, the production process is closer to completion before the leading baryon makes its subsequent collisions, and hence κ decreases as the incident energy decreases. As the energy becomes too low, however, there may be absorption of the produced particles. Careful measurements of κ as a function of energy may allow one to distinguish the different effects.

The success (or partial success) of the present model poses an interesting puzzle which needs resolution in the future. In this model, energy losses occur inside the nucleus, while the fast particles are produced outside the nucleus. What is the space-time picture of the production process before the projectile emerges from the target nucleus? Can the schematic picture of Figs. 1 and 2 be put in a more quantitative form, as in the Lund model of particle production?[56] Or, alternatively, can one speak of a formation zone as suggested by Brodsky and Stodolsky?[39] How does one deduce theoretically the effect of interference of the production process due to subsequent collisions? How does the interference affect the momentum of the colliding incident baryon? These are some of the unanswered questions which need to be resolved. More rigorous theoretical justification of the model will also be of interest.

ACKNOWLEDGMENTS

The author wishes to thank Professor W. Busza for helpful discussions and criticism. He also wishes to thank Dr. M. Shalaby for his interest in the early phase of this work. The research was sponsored by the Division of Nuclear Physics, U.S. Department of Energy, under Contract No. DE-AC05-840R21400 with Martin Marietta Energy Systems, Inc.

[1]J. D. Bjorken, Phys. Rev. D **27**, 140 (1983).
[2]K. Kanjantie and L. McLerran, Phys. Lett. **119B**, 203 (1982).
[3]T. D. Lee, Columbia University Report No. CU-TP-226, 1981 (unpublished).
[4]M. Gyulassy, Lawrence Berkeley Report No. LBL-15175, 1982 (unpublished).
[5]J. Rafelski and M. Danos, NBS Report No. NBSIR 83-2725, 1983 (unpublished).
[6]For example, L. McLerran and B. Svetitsky, Phys. Lett. **96B**, 195 (1981); Phys. Rev. C **24**, 450 (1981); I. Montvay and H. Pietarinen, Phys. Lett. **115B**, 151 (1982); J. Kogut *et al.*, *ibid.* **48**, 1140 (1982).
[7]C. Y. Wong, Phys. Rev. D **30**, 961 (1984).
[8]D. Schramm, and K. A. Olive, in *Quark Matter '83,* proceed-

ings of the Third International Conference on Ultrarelativistic Nucleus-Nucleus Collisions, Brookhaven National Laboratory, 1983, edited by T. W. Ludlam and H. E. Wegner [Nucl. Phys. **A418**, 289c (1984)]; D. Schramm, Fermilab Report No. Conf-83/83-AST (unpublished).

[9]C. Y. Wong, Phys. Rev. Lett. **52**, 1393 (1984).

[10]C. Y. Wong, Phys. Rev. D **30**, 972 (1984).

[11]R. J. Glauber, *Lectures in Theoretical Physics,* edited by W. E. Brittin and L. G. Dunham (Interscience, New York, 1959), Vol. 1, p. 315.

[12]V. N. Gribov, Zh. Eksp. Teor. Fiz. **57**, 1306 (1969) [Sov. Phys. JETP **30**, 709 (1970)]; for a review see L. Bertocchi, Nuovo Cimento **11A**, 45 (1972) and J. H. Weis, Acta Phys. Pol. **B7**, 851 (1976).

[13]R. Blankenbecler, A. Capella, J. Tran Thanh Van, C. Pajares, and A. V. Ramallo, Phys. Lett. **107B**, 106 (1981).

[14]A. Capella and A. Krzywicki, Phys. Lett. **67B**, 84 (1977).

[15]K. Kinoshita, A. Minaka, and H. Sumiyoshi, Prog. Theor. Phys. **63**, 928 (1980); **63**, 1268 (1980).

[16]K. Kinoshita, A. Minaka, and N. Sumiyoshi, Prog. Theor. Phys. **61**, 165 (1979); Z. Phys. **8**, 205 (1981).

[17]J. P. Vary, Phys. Rev. Lett. **40**, 295 (1978); M. Sandel, J. P. Vary, and S. I. A. Garpman, Phys. Rev. C **20**, 744 (1979).

[18]J. Kapusta, Phys. Rev. C **27**, 2037 (1983).

[19]A. S. Carroll *et al.*, Phys. Lett. **80B**, 319 (1979).

[20]J. E. Elias, W. Busza, C. Haliwell, D. Luckey, L. Votta, and C. Young, Phys. Rev. Lett. **41**, 285 (1978); J. E. Elias, W. Busza, C. Haliwell, D. Luckey, P. Swartz, L. Votta, and C. Young, Phys. Rev. D **22**, 13 (1980).

[21]W. Busza, in *Proceedings of the 4th High Energy Heavy Ion Summer Study, Berkeley, 1978* (Lawrence Berkeley Laboratory Report No. LBL-7766), p. 253.

[22]Y. Nambu, lectures at the Copenhagen Symposium, 1970 (unpublished).

[23]A. Capella, U. Sukhatme, C. I. Tan, and J. Tran Thanh Van, Phys. Lett. **81B**, 68 (1979); Chao Wei-qin, C. B. Chiu, He Zuoxin, and D. M. Tow, Phys. Rev. Lett. **44**, 518 (1980); C. B. Chiu and D. M. Tow, Phys. Lett. **97B**, 443 (1980); A. Capella, C. Pajares, and A. V. Ramallo, Nucl. Phys. **B241**, 75 (1984).

[24]H. Aihara *et al.*, Phys. Rev. Lett. **54**, 274 (1985).

[25]D. D. Barton *et al.*, Phys. Rev. D **27**, 2580 (1983).

[26]A. E. Brenner *et al.*, Phys. Rev. D **26**, 1497 (1982).

[27]W. Busza, in *Quark Matter '83* (Ref. 8) [Nucl. Phys. **A418**, 635c (1984)]; W. Busza and A. S. Goldhaber, Phys. Lett. **139B**, 235 (1984).

[28]R. C. Hwa, Phys. Rev. Lett. **52**, 492 (1984); R. C. Hwa and M. S. Zahir, Phys. Rev. D **31**, 499 (1985).

[29]L. Csernai and J. Kapusta, contributed paper to Winter Workshop on Nuclear Dynamics, Copper Mountain, Colorado, 1984 (unpublished).

[30]J. Hüfner and A. Klar, Phys. Lett. **145B**, 167 (1984).

[31]S. Daté, M. Gyulassy, and N. Sumiyoshi, Lawrence Berkeley Laboratory report (unpublished).

[32]I. Otterlund, S. Garpman, and I. Lund, Z. Phys. C **20**, 281 (1983).

[33]M. A. Faessler, Ann. Phys. (N.Y.) **137**, 44 (1981).

[34]K. Gottfried, Phys. Rev. Lett. **32**, 957 (1981).

[35]A. Białas, W. Czyż, and W. Furmanski, Acta Phys. Pol. **B8**, 585 (1977); A. Białas, and W. Czyż, *ibid.* **B10**, 831 (1979); A. Białas, W. Czyż, and L. Lesmiak, Z. Phys. C **13**, 147 (1982).

[36]V. V. Anisovich, Yu. M. Shabelski, and V. M. Shakhter, Nucl. Phys. **B135**, 477 (1978); N. N. Nikolaev, Phys. Lett. **B70**, 95 (1977); G. Berland, A. Dar, and G. Eilam, Phys. Rev. D **22**, 1547 (1980).

[37]S. J. Brodsky, J. F. Gunion, and J. H. Kühn, Phys. Rev. Lett. **39**, 1120 (1977).

[38]C. Y. Wong and T. A. Welton, Phys. Lett. **49B**, 243 (1974); H. H. K. Tang and C. Y. Wong, Phys. Rev. C **21**, 1846 (1980); **26**, 284 (1982).

[39]S. J. Brodsky, Report No. SLAC-PUB-3256, 1983 (unpublished); Report No. SLAC-PUB-3219, 1983 (unpublished); G. T. Bodwin, S. J. Brodsky, and G. P. Lepage, Phys. Rev. Lett. **47**, 1799 (1981); L. Landau and I. Pomeranchuk, Dok. Akad. Nauk. SSSR **92**, 535 (1953); **92**, 735 (1953); L. Stodolsky, Phys. Rev. Lett. **28**, 60 (1972); A. Białas and L. Stodolsky, Acta Phys. Pol. **B7**, 845 (1976).

[40]J. D. Bjorken, in *Lecture Notes on Current-Induced Reactions,* edited by J. Komer *et al.* (Springer, New York, 1975); J. Kogut and L. Susskind, Phys. Rev. D **10**, 732 (1974).

[41]E. A. Schmidt and R. Blankenbecler, Phys. Rev. D **15**, 332 (1977).

[42]T. Eichen *et al.*, Nucl. Phys. **B44**, 333 (1972).

[43]J. Y. Allaby *et al.*, CERN Report No. CERN-70-12, 1970 (unpublished).

[44]F. G. Taylor *et al.*, Phys. Rev. D **14**, 1217 (1972).

[45]Sa Ban Hao and Cheuk-Yin Wong, ORNL report (unpublished).

[46]L. Remsberg *et al.*, in *Proceedings of the 7th High Energy Heavy Ion Study, Darmstadt, 1984* (Gesellschaft fur Schwerionforschung Report No. GSI-85-10), p. 439.

[47]A. Bohr and B. R. Mottelson, *Nuclear Structure* (Benjamin, New York, 1969), Vol. I, pp. 160—162.

[48]E. Albini, P. Capiluppi, G. Giacommeli, and A. M. Rossi, Nucl. Phys. **A32**, 101 (1976).

[49]C. De Marzo *et al.*, Phys. Rev. **29**, 363 (1984).

[50]V. Bakken, F. O. Breivik, and T. Jacobsen, Nuovo Cimento **75A**, 376 (1983).

[51]T. Kafka *et al.*, Phys. Rev. D **16**, 1201 (1977).

[52]B. Andersson, G. Gustafson, and B. Söderberg, Z. Phys. C **20**, 317 (1983).

[53]There are data which contradict Eq. (7.4) (Fig. 2 of Ref. 54). However, the data of $pp \to \pi^- X$ reported there contain events from both of the pp hemispheres and should be divided by a factor of 2 (private communication from V. Bakken). This brings $d\sigma(pp \to \pi^- X) \simeq d\sigma(pn \to \pi^- X)$.

[54]V. Bakken, F. O. Brevik, and T. Jacobson, Nuovo Cimento **68A**, 348 (1982).

[55]K. Heller *et al.*, Phys. Rev. D **16**, 2737 (1977); P. Skubic *et al.*, *ibid.* **18**, 3115 (1978).

[56]B. Andersson, G. Gustafson, and B. Söderberg, Z. Phys. C **20**, 317 (1983).